minerals

MDPI

Article

Distribution and Mode of Occurrence of Co, Ni, Cu, Zn, As, Ag, Cd, Sb, Pb in the Feed Coal, Fly Ash, Slag, in the Topsoil and in the Roots of Trees and Undergrowth Downwind of Three Power Stations in Poland

Henryk R. Parzentny [1,*] and Leokadia Róg [2]

[1] Unemployed, Cooperating with the Institute of Earth Sciences, University of Silesia in Katowice, Będzińska 60, 41-200 Sosnowiec, Poland
[2] Department of Solid Fuels Quality Assessment, Central Mining Institute, Plac Gwarków 1, 40-166 Katowice, Poland; lrog@gig.eu
* Correspondence: hr.parzentny@vp.pl

Abstract: It is supposed that the determination of the content and the mode of occurrence of ecotoxic elements (EE) in feed coal play the most significant role in forecasting distribution of EE in the soil and plants in the vicinity of power stations. Hence, the aim of the work was to analyze the properties of the feed coal, the combustion residues, and the topsoil which are reached by EE together with dust from power stations. The mineral and organic phases, which are the main hosts of EE, were identified by microscopy, X-ray powder diffraction, inductively coupled plasma atomic emission spectrometry, and scanning electron microscope with an energy dispersive X-ray methods. The highest content of elements was observed in the Oi and Oe subhorizons of the topsoil. Their hosts are various types of microspheres and char, emitted by power stations. In the areas of long-term industrial activity, there are also sharp-edged grains of magnetite emitted in the past by zinc, lead, and ironworks. The enrichment of the topsoil with these elements resulted in the increase in the content of EE, by between 0.2 times for Co; and 41.0 times for Cd in the roots of Scots pine, common oak and undergrowth, especially in the rhizodermis and the primary cortex and, more seldom, in the axle roller and cortex cells.

Keywords: ecotoxic elements; coal; fly ash; slag; power station; topsoil; roots

Citation: Parzentny, H.R.; Róg, L. Distribution and Mode of Occurrence of Co, Ni, Cu, Zn, As, Ag, Cd, Sb, Pb in the Feed Coal, Fly Ash, Slag, in the Topsoil and in the Roots of Trees and Undergrowth Downwind of Three Power Stations in Poland. *Minerals* **2021**, *11*, 133. https://doi.org/10.3390/min11020133

Academic Editor: Shifeng Dai
Received: 10 December 2020
Accepted: 25 January 2021
Published: 28 January 2021

1. Introduction

Although the technology of thermal processing of coal and energy generation through combusting coal in power stations (PS) has been developed for decades, it still poses a great threat to the environment due to the emission of solid particles enriched with numerous ecotoxic elements (EE). Coal properties and the technical conditions of combustion determine how toxic the combustion products are. Among the combustion conditions, the most important ones are: the temperature and technology [1,2], fragmentation [3], moisture content, the method of feeding coal into the combustion chamber [3,4], boiler type, and construction of the combustion chamber, among others [4]. Among the properties of coal which determine the content of EE in the combustion residues, the most important ones are the content of and the mode of occurrence of the elements in the feed coal. The qualities/indices of coal were hitherto determined in reference to whole brown coal [5–8] and hard coal in the deposits around the world [7,9–11]; the quality of feed coal was not referred to. It is assumed that binding EE in coal with the organic fraction and sulfide minerals increases the volatility of the elements, which are easily adsorbed on fine particles when the flue gases cool down [2,12–19]. It is totally the opposite with the elements which are connected with minerals other than sulfides. They probably remain in the fly ash matrix or evaporate slowly [16,20]. The finest particles of fly ash [18,21–26], and the dusts

sedimenting on the surface of the soil [24,27,28], may be much more enriched with EE than the feed coal. The sedimenting particles are then subjected to rainwater and surface water. The leachability of elements from the particles depends strongly on the value of pH in the water environment. It is assumed that the increased leachability of EE from the particles of combustion residues may occur when the elements are concentrated on the surface of alkaline particles and they are in the acidic environment of the groundwater (e.g., [29–32]), or when the elements are on the surface of acidic particles in a neutral or slightly alkaline environment of rainwater or standing water (e.g., [29,33]). Although alkalinity weakens the potential to extract a significant amount of EE, it increases the mobility and leachability of a few oxyanionic species (B, V, Cr, As, Se, Mo, Sb, and W). The concentration ratio of Ca and S in the fly ash probably determines the pH of the water–ash system and plays a crucial role in assessing its ability to leach most of the elements contained in the fly ash [29]. The leachability is then dependent on the mode of occurrence of the elements in the feed coal and in the crystalline structure of the fly ash [34].

Ecotoxic elements occurring in the topsoil and in the groundwater may easily become bioavailable and then they can reach the underground and the above-ground portions of plants [35]. The bioavailability of plants depends, among other things, on the speciation of the elements [36,37]; the physical, chemical and biological properties of the soil, including the pH value, cation exchange capacity, redox potential, the content of organic coal; as well as on the nature of a given element [37–39]. It is assumed that Cd, Cu, and Co, together with Fe and Mo, are elements which are accumulated in a greater amount in the roots, but some of them are transported to the shoots. In turn, Pb, Sn, and Ag, together with Ti, Zr, Cr, V, and Ga, concentrate mainly in the roots, and only small amounts of them are transported to the shoots; while Zn, Ni, and Mn reach comparable concentrations in the roots and shoots [37]. The toxic influence of these elements on plants include on, among others, hinders the blooming, growth and maturing of gametophytes, the development of germs, the germination of seeds and the development of seedlings [40,41]. It is manifested through leaf and needle scorch, dwarfism, and wilting (e.g., [37,42]). Ecotoxic elements, upon reaching edible plants, give them toxic characteristics. As a result, the plants, if consumed, pose a threat to people and animals, often causing diseases, or even leading to death.

In the vast literature of the last decade dedicated to research into the types of soil exposed to particulate emissions of technogenic origin, the high content of EE is often observedin the topsoil in the surroundings of: ore mines (e.g., [43,44]) and coal mines (e.g., [45]), ironworks (e.g., [46,47]) or nonferrous metal smelters (e.g., [48]), brick factories [49], petrochemical plants [50], cities (e.g., [51–53]), industrial districts (e.g., [54–56]), and reservoirs (e.g., [57]) and mining waste disposal sites (e.g., [58,59]). The Co, Ni, Cu, Zn, As, Cd, and Pb contents in the topsoil were also determined in the vicinity of PS, burning brown coal (e.g., [60–62]) and/or bituminous/hard coal. Topsoil is most often considered as one horizon of topsoil, which has been studied in agricultural [63–67], urban [68–70], savanna [71], industrial [72–75], and ustalf [76] ares, and occasionally as two or more horizons of topsoil [77–80]. In each of the works, the highest content of EE was observed in the topsoil downwind of the emitters, without analyzing the affiliation to given genetic horizons/subhorizons of soil. No publications were found determining the mode of occurrence of EE in the organic or mineral (both magnetic or nonmagnetic) fraction of the topsoil

The aim of this work was to determine the content distribution and the mode of occurrence of selected trace elements (Co, Ni, Cu, Zn, As, Ag, Cd, Sb, Pb) in feed coal, in the combustion residue, in given horizons/subhorizons of the topsoil, and in the roots of trees and undergrowth downwind of the power stations combusting solely bituminous coal. This paper considers the elements that various authors believe (e.g., [5,38,81,82]) to be potentially ecotoxic and harmful, that the content of which is considered to be enriched [83–86] in the Upper Silesian Coal Basin coal (where the feed coal comes from), and that melting points lower than the coal combustion temperature in PS (i.e., Ni, Cu, Zn, As, Ag, Cd, Sb, Pb). It is possible that the results of the presented research will help in selecting methods for the

preparation of EE-free coal, in identifying the layers of soil which are most polluted with EE, qualifying them for removing or modifying, and choosing plants which will be able to colonize the soil. Additionally, based on the calculated enrichment factor and the average content of EE in feed coal, it will be possible to assess the EE content in the soil horizons.

2. Materials and Methods

2.1. Studied Area and Materials

There was an interest in power stations located in areas of diversified industrial load and building density in different regions of Poland (Figure 1). The selected PS combusted coal from the same Upper Silesian Coal Basin, but independently purchased. Feed coal is combusted in coal dust-fired steam boilers at an average temperature of 1475 °C. The wet methods of flue gas desulfurization applied in the PS do not result in any contact between the fly ash, the slag, and the sorbent. In PS-a, PS-b, and PS-c, there were collected: three whole feed coal samples, three whole fly ash samples and three whole slag samples (one sample from each PS). Each sample of feed coal, fly ash and slag consisted of six partial samples, collected every 15 min. The samples of feed coal were collected from the feeder directly before combustion. The fly ash samples were collected from the hoppers under the electrostatic precipitators, and the slag samples were collected from the slag scrapers. The samples of whole feed coal, fly ash, and slag were averaged, and then representative laboratory samples were selected.

The forest areas, located in the vicinity of the power stations (Figure 1), where soil, tree roots, and undergrowth samples were taken, are:

- Area A; high density of pine forests adjoining Kozienice Landscape Park [87]. In this area there are few towns, with a maximum population of 17,500 people. In area A, except PS-a, there are no other industrial emitters of particulates. The power station started operating in 1972. Currently, it generates energy of approximately 4000 MW. The soil samples were collected between 7.7 km and 13.1 km NE, E, and S of the PS-a.
- Area B is burdened with many years of industrial activities (coking plants, hard coal mines, zinc and lead ore mines, steel and zinc works, small PS, chemical plants) and 19 neighboring cities, with a total population of 2.013 million people, forming the Upper Silesian conurbation [88]. PS-b is located in this area, which has been combusting feed coals since 1954; and, currently, it generates energy of approximately 220 MW. In area B, oak and pine trees prevail.The soil samples were collected between 9.9 km and 12.9 km NNE and NE of PS-b.
- Area C includes mainly pine forests adjoining landscape conservation areas (Stobrawa—Turawa Forests, Niemodlin Forests). It includes a few towns and villages with a total population of 9800 people and a few small industry plants [89]. In area C, there is a coal-fired power station (PS-c), operating since 1993, which generates energy of approximately 1500 MW. Opole is located approximately 12 km south of area C (118,300 people). In the area, there were no and there are no metal works and no other power stations. The soil samples were collected at a distance between 5.2 km and 11.1 km NNE and E of PS-c.

In research areas A, B, and C, in nine places located between 5.2 km and 13.1 km from the emitter, following the main wind directions (Figure 1) downwind of the PS, three whole soil samples were collected. Each of the samples consisted of eight cores collected from the top layer of soil (approximately 30 cm) within approximately 1 m diameter. The soil samples were collected with a plastic riverside auger. The genetic horizons and subhorizons of the soil were identified and characterized, following the current standards of the World Reference Base and Soil Taxonomy [91,92]. The whole soil samples from given soil horizons and subhorizons were dried at the temperature of 50°C. Then, in each soil core, the fine roots of the trees and the undergrowth were sorted and cleaned of soil particles. Seven pooled samples of the roots of Scots pine (*Pinus sylvestris* L.), the undergrowth (mainly European blueberry (*Vaccinium myrtillus*), lingonberry (*Vaccinium vitis-idea*), and bracken

(*Pteridium aquilinum*)), and two samples of the roots of common oak (*Quercus robur* L.) and the undergrowth (as above) were obtained.

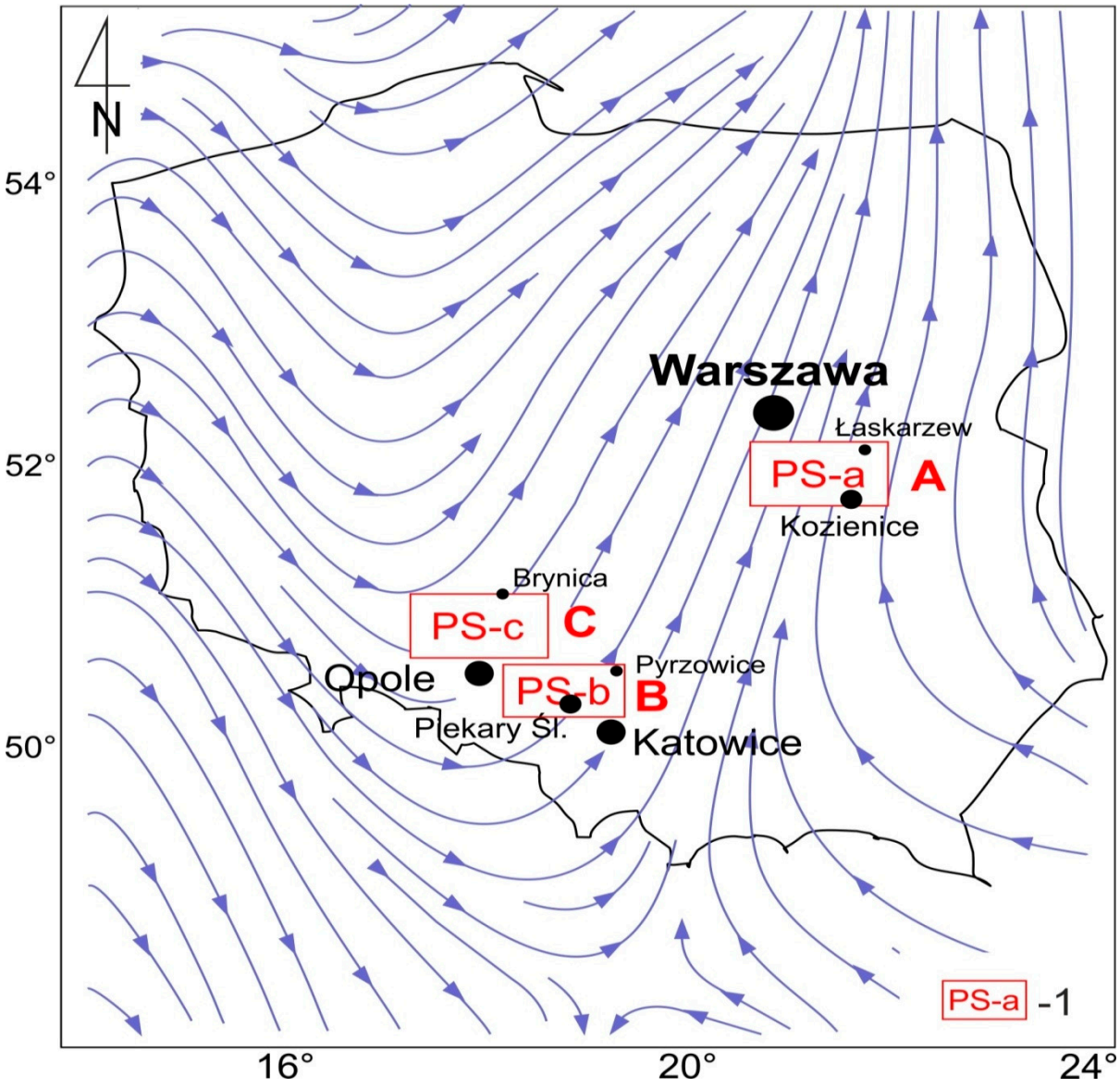

Figure 1. Location of research areas and power plants in comparison with the main wind directions in Poland (after: [90]). 1—power station in areas (e.g., A; there is no consent to enter the name).

2.2. Research Range, Methods, and Calculations

The samples of the whole feed coal and the slag were ground in an agate mortar into <0.2 mm grains. The obtained samples were sorted with a portable magnetic separator into magnetic and nonmagnetic fractions; the yield of the fraction was determined (see Table S1). The whole fly ash samples were sorted with polyurethane sieves into particle classes of the equivalent spherical diameter of: >0.5 mm, 0.5–0.2 mm, 0.2–0.05 mm, and <0.05 mm. Each of the granulometric particle classes was then sorted with a portable magnetic separator into magnetic and nonmagnetic fractions; the fraction yield was determined (Table S1). Each layer of soil representing a horizon/subhorizon of soil was sorted with a portable magnetic separator into magnetic and nonmagnetic fractions; the yield of the obtained fractions was calculated (Table S2).

The petrographic composition and reflectance of the whole feed coal was determined with the Zeiss Axio Imager D1m microscope (40× objective, 10× oculars, and 546 nm interference filters, reflected white light, immersion oil) with an integration table, following the standards specified by the ICCP and the procedures described in ISO 7404-3 [93] and ISO 7404-5 [94]. The composition of the mineral matter of the feed coal was verified with Bruker's D8 Discover X-ray powder diffractometer (iron filtered CoKα radiation, Ni-filter, and Lynxeye detector). The XRD pattern was recorded at an interval of 2θ 2.6–70°, every 0.01°. The calculations of the content of given mineral phases were conducted with Diffrac v. 3.0 Bruker AXS software following the Taylor method [95], based on the profiling diffractogram [96]. Ruan and Ward [97] and Mahieux et al. [98] presented implementation of the method for materials containing carbon. The results are shown in Table 1.

The samples of granulometric grain classes and fractions of the feed coal, fly ash, slag and soil, as well as the samples of the roots were sent to the analytical laboratory AcmeLab (presently Bureau Veritas Commodities Canada Ltd.) in Vancouver, Canada. Like Guo et al. [99] and Silva et al. [100], the content of the Co, Ni, Cu, Zn, As, Ag, Cd, Sb, and Pb was determined with atomic emission spectroscopy (multi-acid ICP-AES). Each sample (0.25 g) was subjected to complete dryness with an acid solution (2:2:1:1) of H_2O-HF-$HClO_4$-HNO_3. Then 50% HCl was added to the residue and heated with a hot mixing block. After cooling, the solutions were transferred to test tubes and made up using dilute HCl. Standard references used for ICP-AES are included in Oreas 45E 2017.1, OREAS25a, Oreas25A-4A COA 2019.2, Oreas45E, and OREAS45H [101]. The results of the chemical analysis are presented in the Table 2 and in Supplementary materials (Tables S1 and S2).

With Pearson's chi-squared test, the Kolmogorov–Smirnov test, and the Shapiro–Wilk test (with a significance level of $\alpha = 0.05$), the hypothesis concerning the normal distribution of results of the conducted measurements was verified. Then, there were calculated:

- The average values of the content of elements in the analyzed feed coal, in the combustion residue, in the soil, and in the roots were compared with hard coal Clarke values [6] and with the average content of elements in global cambisols [38];
- The share of grain size classes and of magnetic and nonmagnetic fractions in the fly ash and the share of magnetic and nonmagnetic fraction in the feed coal and the slag in concentrating elements in the whole fly ash, whole feed coal, and whole slag. To do this, the percentage share of each of the components of the weighted average in the total value of the weighted average was calculated. The weighted average component is the product of the element content in each class of fly ash grains and in each slag fraction, as well as the percentage mass share of each class and grain fraction in the composition of whole fly ash and in the whole slag. The calculations were made according to the Equations (1) and (2) and their results are presented in Figure 2 (see Table S1);
- The share of the horizon/subhorizon of soil (sorted into magnetic and nonmagnetic fractions) in concentrating elements in the whole topsoil of 30 cm thickness. To do this, the percentage share of each of the components of the weighted average was calculated. The component is the product of the content of a given element in each fraction of soil horizon/subhorizon and the percentage share of the weight of each fraction of soil horizon/subhorizon in the composition of the whole topsoil. The total of the components of the weighted average is 100%. The calculations were made according to the Equations (1) and (2) and their results are presented in Figure 3 (see Table S2).

$$x_w = s_1 + s_2 + \ldots + s_n = 100(wt\ \%)s_n = x_n w_n \quad (1)$$

$$s_n(wt\%) = s_n * 100/x_w \quad (2)$$

where x_w issum of the components of the weighted average; x_n is element content in n fraction of the feed coal or fly ash or slag or soil horizon/subhorizon; w_n is weight of the fraction/100.

In the samples (samples of granulometric fly ash classes, samples of magnetic and nonmagnetic fraction of feed coal, fly ash grain-size classes, slag, and horizons/subhorizons of soil) with the highest content of the elements and in the roots, the content of Co, Ni, Cu, Zn, As, Ag, Cd, Sb, and Pb in the microarea of mineral particles and organic matter was determined. The analysis was conducted with ascanning electron microscope (SEM/EDS) on polished microsections. The microscope used was aHitachi SU-3500, with ThermoFisher Scientific energy dispersive X-ray UltraDry EDS Detector. Standard conditions were maintained to conduct the analyses (acc. voltage = 15.0 kV, bse-comp = 30 Pa, image resolution = 1024 by 768, image pixel size = 0.04–0.27 μm, magnification = 90–5000). The results of the analyses are presented in Table 3 (see Table S3), and the examples of interesting analyses are presented in Figure 4.

To check if the content of EE in the samples of fly ash, slag, and soil may be treated as dangerous for the environment, they were compared with the permissible values for the soil group (Table 2). Following the regulation of the Polish Ministry of Environment on the criteria of colliery spoil classification [102] based on the European Union's regulation [103], it was assumed that the combustion residues of the analyzed feed coal and soil in the vicinity of a power station may be considered to be neutral for the environment if the content of the elements in the samples does not exceed the quality thresholds for soil or land specified for the soils of group I. The group refers to agricultural soils, forests, built-up areas and urbanized areas (except industrial ones), barren lands and spoils, and road transport infrastructure [104]. The values of PCS are collected and presented in Table 2.

To observe the changes in the content of EE between the coal and the plant roots, the enrichment factor, which expresses the ratio of the element content in the granulometric classes of fly ash, in the magnetic fractions of slag, in the soil horizons/subhorizons and the roots (undergrowth and trees) and the element content in the feed coal, was calculated The results of the calculations are presented in Figure 5 (see Table S4).

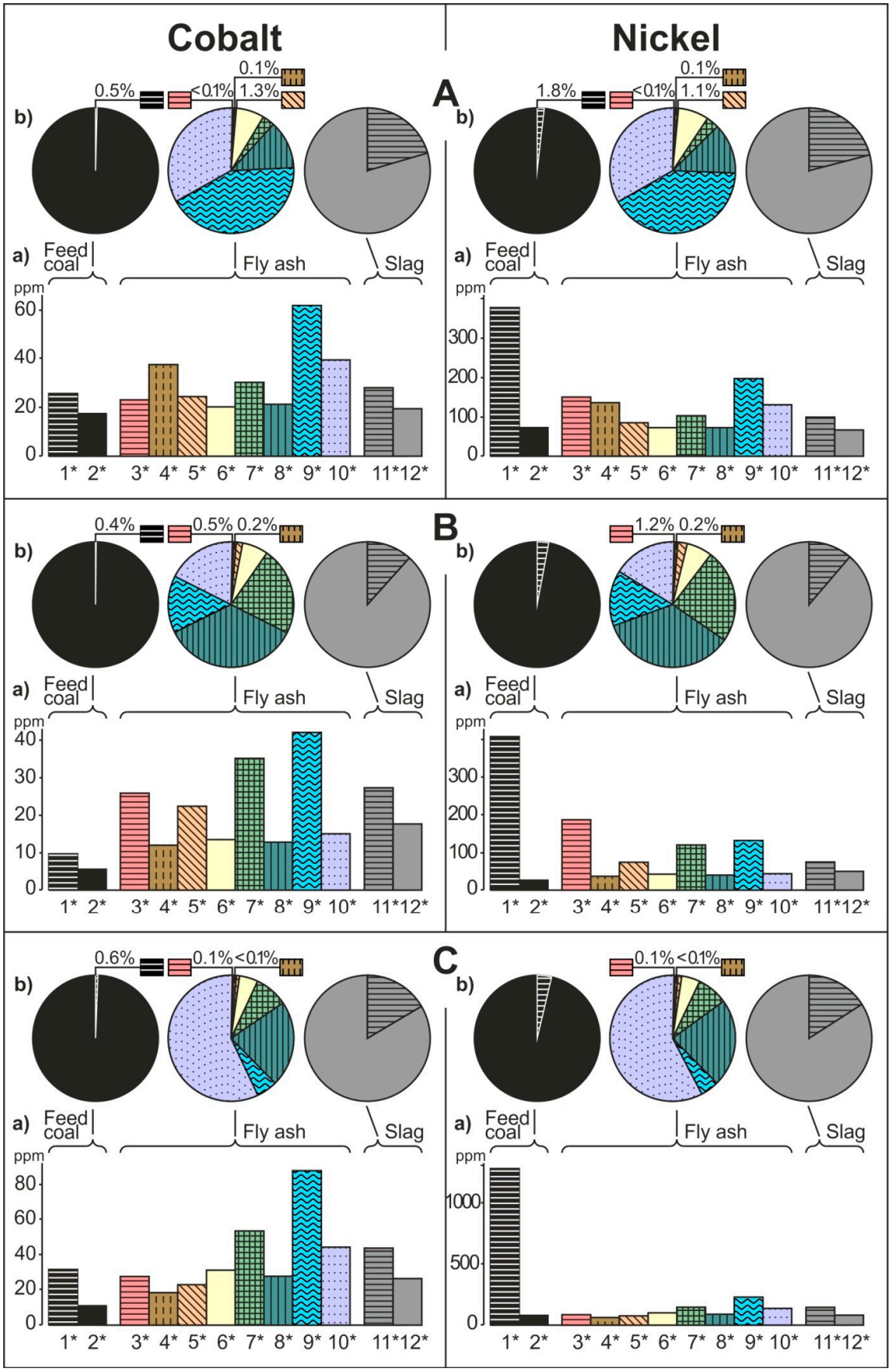

Figure 2. *Cont*.

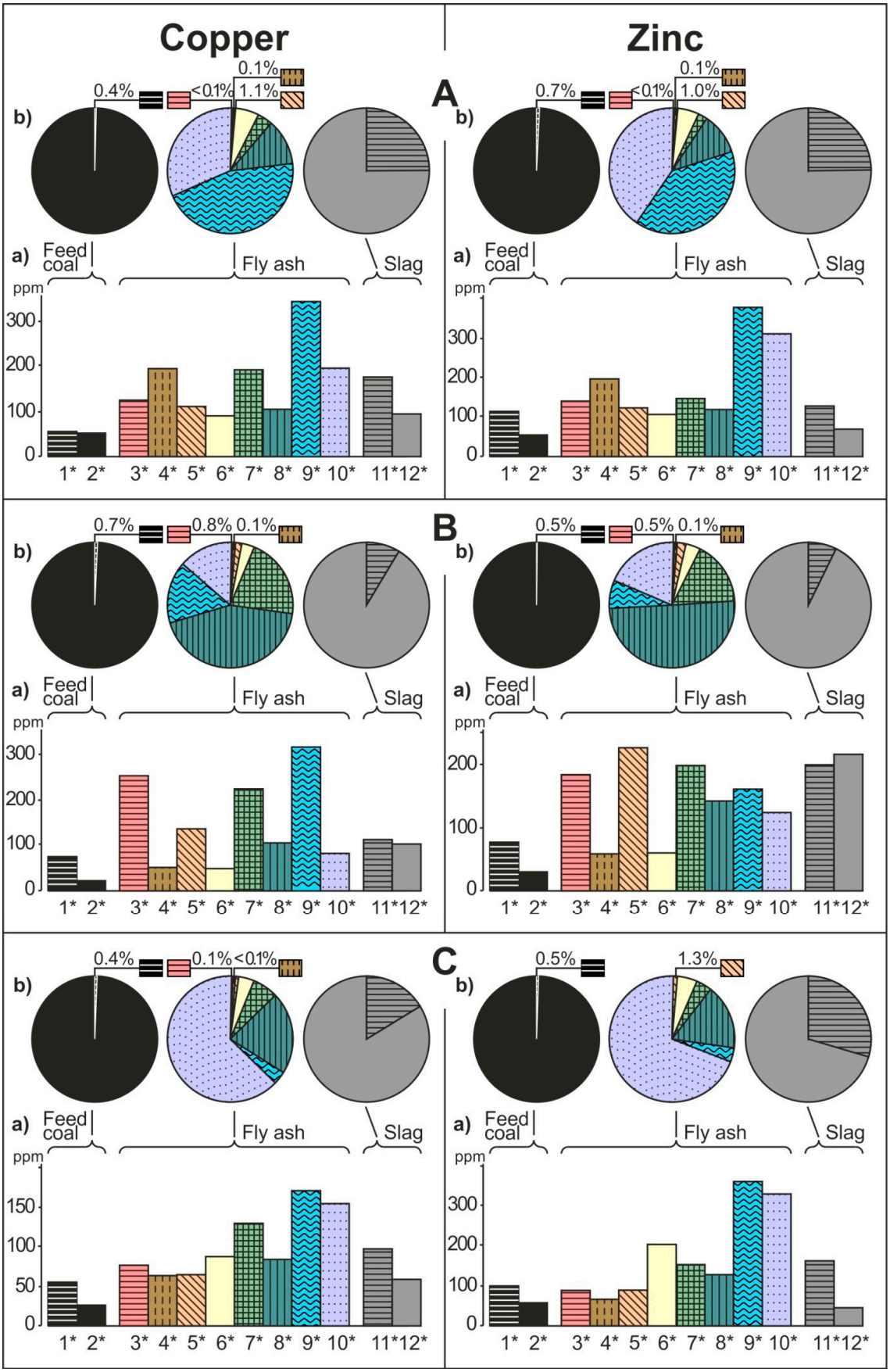

Figure 2. *Cont.*

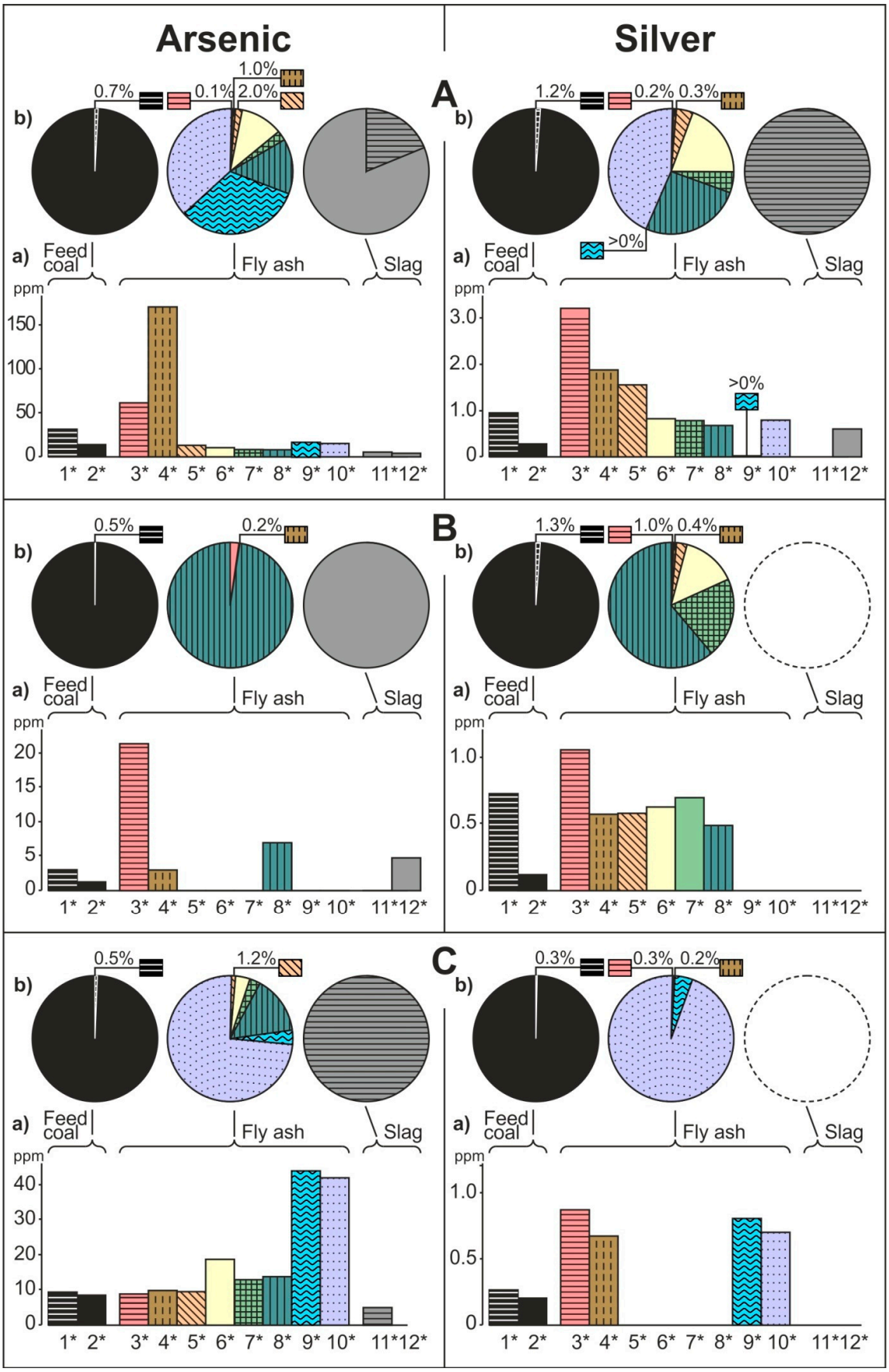

Figure 2. *Cont.*

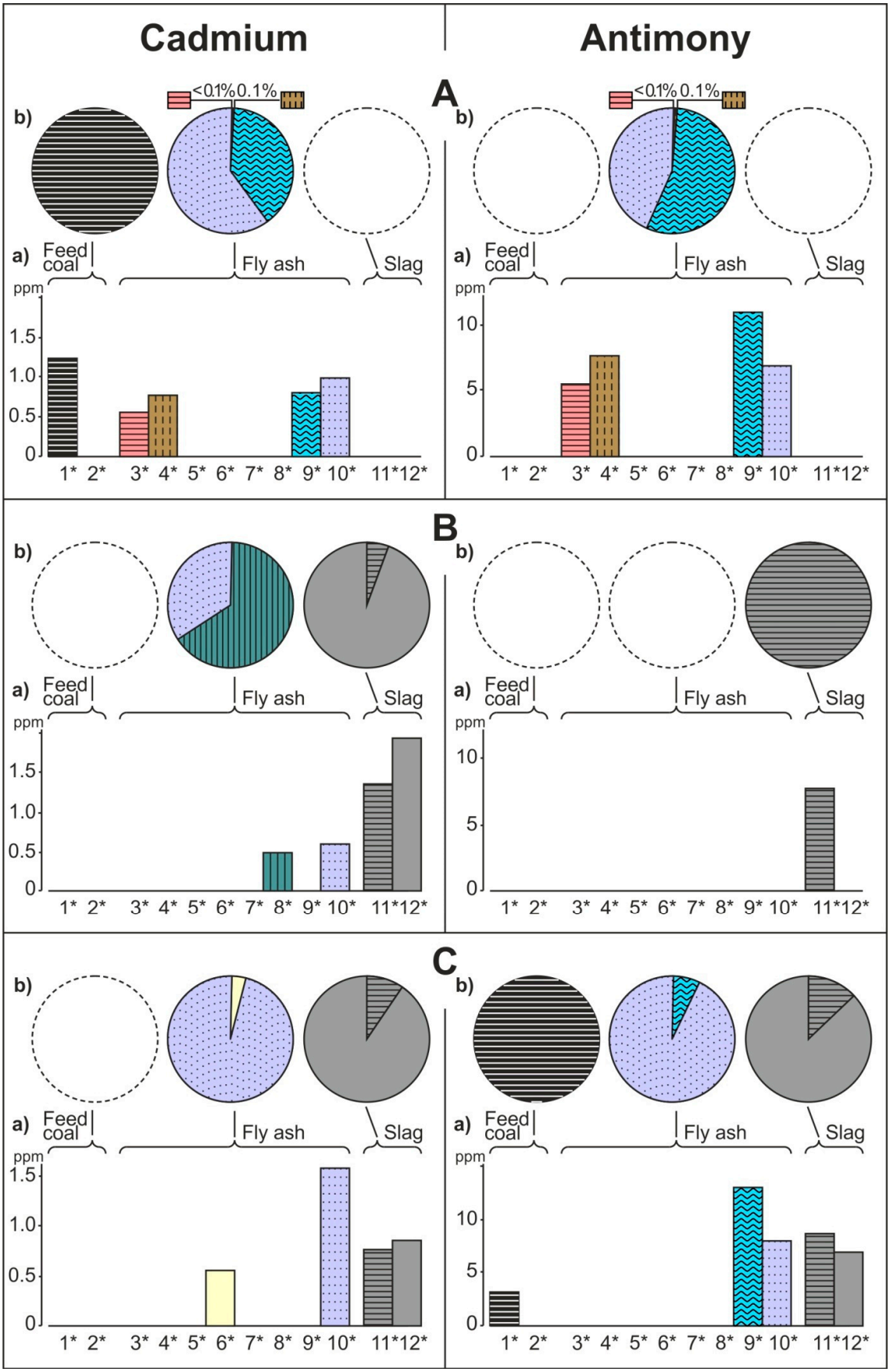

Figure 2. *Cont*.

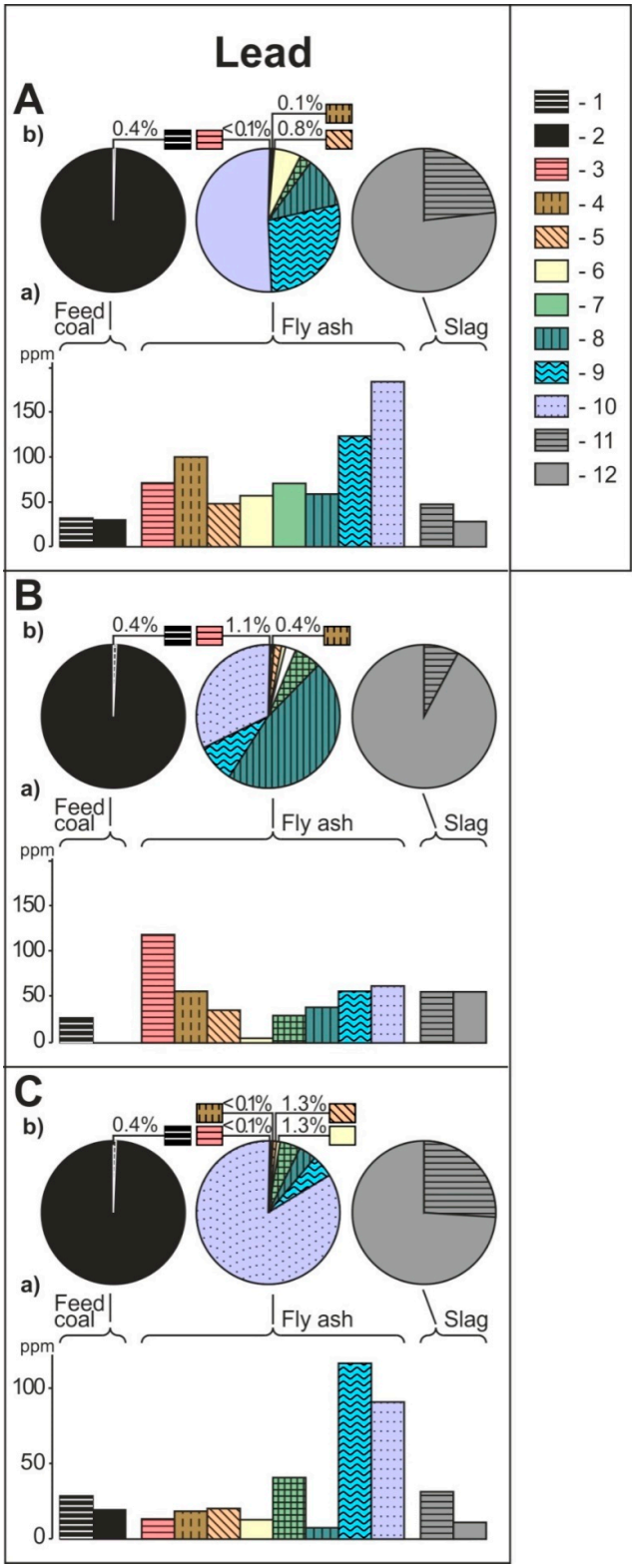

Figure 2. The distribution of element content in the feed coal, fly ash and slag (**a**) and their proportion in determining the average element concentration in the whole feed of coal, fly ash and slag (**b**). * Fractions: 1—magnetic and 2—nonmagnetic fraction of the feed coal, 3–10 fly ash: (3—magnetic and 4—nonmagnetic fraction >0.5 mm, 5—magnetic and 6—nonmagnetic fraction 0.5 ÷ 0.2 mm, 7—magnetic and 8—nonmagnetic fraction 0.2 ÷ 0.05 mm, 9—magnetic and 10—nonmagnetic fraction <0.05 mm), 11—magnetic and 12—nonmagnetic fraction of the slag.

3. Results

3.1. General Petrographic and Geochemical Characteristics of the Subject of the Research

Due to vitrinite reflectance (R_r = 0.81–0.92, Table 1), the feed coal combusted in PS-a, PS-b, and PS-c (Figure 1) was classified (after International Classification of Seam Coals, Final Version [105]) as orthobituminous coal. The feed coal consisted mainly of vitrinite (52.0–66.0%). Its mineral matter (9.3–20.8%) consisted mainly of kaolinite, and secondarily of pyrite, dolomite, and siderite (Table 1).

Table 1. Petrographic characteristics of the whole feed coal from the power plants A–C.

Object/Formula	A	B	C
(In vol. %)			
Vitrinite	66.0	62.8	52.0
Liptinite	2.1	5.0	6.0
Inertinite	11.1	22.9	23.0
Pyrite/FeS_2	5.8	2.0	3.8
Magnetite/$Fe^{2+}Fe^{3+}{}_2O_4$	0.2	0.1	0.3
Hematite/Fe_2O_3	<0.1	<0.1	not found
Quartz/SiO_2	0.1	0.1	1.4
Feldspar/$KAlSi_3O_8$-$NaAlSi_3O_8$-$CaAl_2Si_2O_8$	<0.1	<0.1	<0.1
Apatite/$Ca_5(PO_4)_3$(F,Cl,OH	not found	not found	<0.1
Chlorite/$(X,Y)_{4–6}(Si,Al)_4O_{10}(OH,O)_8$; X and Y = Fe^{+2}, Fe^{+3}, Mg^{+2}, Mn^{+2}, Ni^{+2}, Zn^{+2}, Al^{+3}, Li^{+1}, or Ti^{+4}	not found	not found	<0.1
Kaolinite/$Al_2Si_2O_5(OH)_4$	8.8	4.0	4.1
Illite+muscovite/$K_{0.65}Al_{2.0}[Al_{0.65}Si_{3.35}O_{10}](OH)_2$-$KAl_2(AlSi_3O_{10})(OH)_2$	0.1	0.1	1.9
Calcite/$CaCO_3$/	not found	not found	not found
Dolomite/$CaMg[CO_3]_2$	not found	2.7	7.0
Ankerite/$Ca(Fe^{2+}, Mg, Mn)(CO_3)_2$	not found	0.1	not found
Siderite/$Fe^{2+}CO_3$	5.8	0.2	0.5
Gypsum/$CaSO_4$*$2H_2O$)	not found	not found	not found
Reflectance (%)	0.92	0.81	0.81
Ash yield (wt %)	43.92	11.38	24.57

In comparison with the coal Clarke values [6], the values of Ni, Cu, Zn, and Pb content in the feed coal from power stations PS-a, PS-b, and PS-c; Co, As, and Ag content in the feed coal from power station PS-a; and Co and Ag content in the feed coal from power station PS-c are higher; while Cd and Sb content in the feed coal from power station PS-a–PS-c; Co, As, and Ag content in the feed coal from power station PS-b; and As content in the feed coal from power station PS-c are lower than or similar to the coal Clarke values (Table 2). The feed coal combusted in PS-a has the highest content of the elements and the feed coal combusted in PS-b has the lowest content of the elements.

Most often, the fly ash consists of0.05–0.2 mm (PS-b) and <0.05 mm (PS-a and PS-c) nonmagnetic particles. The slag also consists of nonmagnetic particles (see Table S1). The values of the content of the elements (Co, Ni, Cu, Zn, As, Ag, Cd, Sb, Pb) in the fly ash and in the slag generally do not differ from the content in the fly ash and the slag hitherto measured in other power stations in Poland [106,107], the north-east of Spain [108], India [16], Turkey [21,109], and China [25,110] (Table 2). The content of Co, Ni, Cu, Zn, Ag, and Pb in the fly ash and the Co content in the slag are the highest (similarly to the feed coal) in the combustion residues from PS-a, and the lowest in the residues from PS-b. The content of As, Cd, and Sb in the fly ash and the content of Ni, Cu, Zn, As, Ag, Cd, Sb, and Pb in the slag is disproportional to the content of the elements in the feed coal combusted in PS-a–PS-c. In comparison with the permissible concentrations of EE in the soils or the ground defined for group I of soils (according to the Polish Journal of Laws 2016 item 1395; [104]), the average content of the elements in the analyzed fly ash and slag from power stations PS-a, PS-b, and PS-c is generally lower (Table 2, see Table S1). An exception to this tendency is the above-standard average content of As in the fly ash from PS-c.

The identified structure of the topsoil indicates that, in the studied area, there are cambisols (Figure 3, see Table S2). In most of the analyzed points around the power stations, the organic horizon (2.0–7.3 cm thick) consists of three thin subhorizons (Oi, Oe, and Oa (Figure 3, see Table S2)), and horizon E does not occur in any of the points. Horizon Ah (5.8–12.0 cm thick) consists of homogenized and transformed organic matter, co-occurring with sand. Horizon B (12.8–20.0 cm thick) is formed of yellow and light-brown sand containing clay and iron. The total content of Co, Ni, Cu, and As in the topsoil is lower, and the content of Zn, Ag, Cd, Sb, and Pb in the topsoil is higher than in cambisols around the world (after [38]) (Table 2). Among the studied areas, the highest content of Co, Ni, Cu, Ag, and Sb in the topsoil was observed in area A, with PS-a combusting the feed coal of the highest content of the aforementioned elements. In turn, the highest content of Zn, As, Cd, and Pb in the topsoil was observed in area B, where the feed coal of the lowest content of the analyzed elements is combusted. Such high enrichment of the topsoil with Zn, As, Cd, and Pb is probably caused by Zn, Cd, and Pb smelting activities in the past. Moreover, it was observed that the highest content of Zn and Pb in the topsoil (which was observed in area B) is significantly higher, and the content of Co, Ni, Cu, As, Cd, and Sb in the topsoil in each of the studied areas is similar to the content of the elements in the topsoil in the vicinity of the power stations around the world presented in Table 2 (combusting only bituminous/hard coal). Comparing the determined content of the elements in the topsoil in studied areas A–C with the permissible EE concentrations in soils or ground defined for group I of soils (after the Polish Journal of Laws 2016 item 1395; [104]), no excessive content of the elements in the soil in area A and C was observed (except As in the magnetic fraction of horizon B in area C; Table 2, see Table S2). Whereas in the topsoil in area B, there are often observed excessive values of the content of the elements.

Table 2. Element content (g/Mg or ppm) in studied feed coal, fly ash, slag. soil, and roots, compared to the results of other authors and to the Polish Journal of Laws 2016 item.

Element	Object	Sample from Studied Areas			Research Results of Other	PCS **
		A	B	C	Authors *	
Co ***	1 ****	17.1	5.5	10.3	6.0 ± 0.2 [1]	
	2	37.6	17.9	38.5	44.6 [2], 14.6 [3]	
	3	20.4	18.3	27.5	12.0 [3], 15 [4]	
	4	10.1	3.3	0.1	World cambisols 10 [5]	50
	Topsoil in the vicinity of the PS				38.5 [16], 4.8 [7], 18.0 [8], 1.4 [9], 0.9 [10]	
	5	2.5	2.6	0.8	nd *****	
Ni	1	72.3	28.2	72.7	17 ± 1 [1]	
	2	123.7	58.2	111.5	138.8 [2], 35.5 [3], 97.3 [11]	
	3	70.5	52.6	77.4	33.2 [3]	
	4	15.0	7.7	1.4	World cambisols 26 [5]	150
	Topsoil in the vicinity of the PS				52.4 [16], 21.8 [7], 30.3 [8], 2.9 [9], 2.4 [10], 36.0 [12], 3.5 [13], 40.4 [14], 73 [15]	
	5	40.3	8.8	4.6	1.85 [6]	
Cu	1	51.0	20.4	25.8	16 ± 1 [1]	
	2	196.6	124.4	123.2	123.4 [2], 72 [17]	
	3	106.1	101.3	63.1	35.7 [3], 41.0 [18]	
	4	10.1	9.4	2.3	World cambisols 23 [5]	200
	Topsoil in the vicinity of the PS				70.4 [16], 12.3 [7], 40.3 [8], 1.7 [10], 35.6 [12], 33.9 [14], 0.6 [19], 28.0 [20], 8.1 [21]	
	5	21.9	32.9	7.3	1.2–3.5 [5]	
Zn	1	53.9	29.6	58.9	28 ± 2 [1]	
	2	245.8	139.6	242.4	199.2 [2], 282 [4],148 [18]	
	3	77.1	214.3	58.7	31.7 [3], 317 [4], 79.0 [18]	
	4	48.5	221.0	17.7	World cambisols 60[5]	500
	Topsoil in the vicinity of the PS				148.5 [16], 56.1 [7], 124.7 [8], 715 [9], 0.9 [10],33.4 [12], 83.0 [14], 0.7 [19], 34 [21]	
	5	81.9	582.7	369.7	nd	

Table 2. *Cont.*

Element	Object	Sample from Studied Areas			Research Results of Other	PCS **
		A	B	C	Authors *	
As	1	14.4	1.1	8.3	9.0 ± 0.7 [1]	
	2	13.6	3.5	28.5	28.2[2], 60.0 [17], 24.8 [22]	
	3	4.8	4.3	0.5	0.17[3], 19.6 [17], 7.0 [22]	
	4	5.0	8.4	1.8	World cambisols 8.4 [5]	25
	Topsoil in the vicinity of the PS				3.5 [16], 5.1 [12], 17.8 [13], 6.7 [14], <0.1 [19], 12.0 [20]	
	5	<0.1	8.6	19.2	1.96 [6]	
Ag	1	0.3	0.1	0.2	0.090 ± 0.016 [1]	
	2	0.6	0.4	0.4	0.7 [2], 0.8 [3]	
	3	0.1	<0.0	<0.0	0.6 [23]	
	4	4.4	3.0	3.5	World cambisols 0.1 [5]	nd
	Topsoil in the vicinity of the PS				nd	
	5	3.5	1.4	2.2	nd	
Cd	1	<0.01	<0.01	<0.01	0.20 ± 0.04 [1]	
	2	0.52	0.37	0.83	0.9 [2], 0.8 [3], 0.7 [4], 1.3 [17]	
	3	<0.01	1.89	0.85	0.6 [3], 0.5 [4], 0.6 [17]	
	4	0.03	2.55	0.07	World cambisols 0.45 [5]	2.0
	Topsoil in the vicinity of the PS				0.45 [5], 1.08 [16], 0.33 [7], 2.94 [9], 0.08 [10], 0.69 [13], 3.85 [14], 0.01 [15], 0.58 [20], 0.10 [21]	
	5	0.80	4.53	0.72	0.28 [6]	
Sb	1	<0.01	<0.01	0.01	1.00 ± 0.09 [1]	
	2	5.00	<0.01	4.30	7.9[2], 5.8 [4], 3.8 [17]	
	3	<0.01	0.61	7.03	4.3 [4], 2.0 [17], 0.6 [18]	
	4	1.49	0.38	0.99	World cambisols 0.62 [5]	nd
	Topsoil in the vicinity of the PS				1.14 [21]	
	5	<0.01	4.67	0.38	nd	

Table 2. *Cont.*

Element	Object	Sample from Studied Areas			Research Results of Other	PCS **
		A	B	C	Authors *	
Pb	1	34.8	12.2	18.8	9.0 ± 0.7 [1]	200
	2	114.3	40.3	54.2	196.8 [2], 52.0 [3], 48 [4], 66.0 [7]	
	3	30.2	55.3	12.4	31.0 [3], 61 [4], 16.3 [7], 23.0 [10]	
	4	35.2	178.2	16.5	World cambisols 28 [5]	
	Topsoil in the vicinity of the PS				26.6 [16], 13.5 [7], 39.7 [8], 138 [9], 1.3 [10], 18.9 [12], 13.7 [13], 46.9 [14], 33.7 [20]	
	5	28.2	455.8	32.6	0.1–0.3 [16], 11.64 [8]	

* Citations after: [1]—Ketris and Yudovich [6], [2]—Ratajczak et al. [106], [3]—Bhangare et al. [16], [4]—Karayigit et al. [109], [5]—Kabata-Pendias [38], [6]—Lin et al. [111], [7]—Hajduk et al. [67], [8]—Lu et al. [68], [9]—Adeyi and Torto [69], [10]—Kovalchuk et al. [75], [11]—Wierońska et al. [107], [12]—Zhai et al. [63], [13]—Agrawal et al. [65], [14]—Sengupta et al. [66], [15]—Pastrana-Corral et al. [78], [16]—Mandal and Sengupta [112], [17]—Llorens et al. [108], [18]—Vassilev et al. [21], [19]—Howladar et al. [73], [20]—Huang et al. [74], [21]—Parzentny [79], [22]—Wei et al. [110], [23]—Dai et al. [25]. ** Permissible concentrations of EE in soils or ground defined for group I soils. after the Polish Journal of Laws 2016 item 1395 [104]. *** Detection limit of elements in the sample solutions (g/Mg, ppm): Co = 0.2, Ni, Cu, Ag, Cd, Sb, and Pb = 0.1, Zn and As = 1.0 [101]. **** 1—Feed coal. 2—fly ash. 3—slag. 4—cambisols. 5—tree and undergrowth roots. ***** no data.

Table 3. Maximum content (wt %) of element in feed coal, fly ash, slag, topsoil, and undergrowth roots from power stations and in tested areas obtained by the scanning electron microscope (SEM/EDS) method.

Element	Area	Feed Coal		Fly Ash		Slag		Topsoil		Root	
		Cn **	Compound	Cn	Compound	Cn	Compound	Cn	Compound	Cn	Compound
Co	A *	0.13	Anhedral pyrite	0.12	Al-Si crassisphere with Fe	0.22	Apatite on microsphere	0.34	Fe-oxide in cenosphere	0.17	Primary cortex
	B *	0.22	Hematite with siderite	0.08	Calcimagnesiaferrosphere	0.14	Cenosphere	0.27	Ferrosphere	0.11	Primary cortex
	C *	0.45	Fusinite with siderite	0.07	Fe-oxide on ferrosphere	0.07	Al-Si-Fe crassinetwork	0.34	Ca-Mg-Fe-Mn carbonate	0.14	Rhizodermis
Ni	A	0.17	Cassiterite with maceral	0.34	Fe-oxide on microsphere	0.27	Fe-oxide on microsphere	0.30	Organic matter	0.36	Primary cortex
	B	1.63	Hematite skeletal	0.32	Fe-oxide on microsphere	0.16	Magnetite? grain	0.39	Barite	0.11	Primary cortex
	C	4.44	iron oxide grain	0.42	Fe-oxide on cenosphere	1.32	Al-Si-Fe crassinetwork	3.46	Siderite after hematite	0.60	Primary cortex
Cu	A	1.51	Cassiterite with maceral	1.51	Fe-oxide on cenosphere	0.22	Fe-oxide on cenosphere	0.51	Fe-oxide in cenosphere	0.18	Rhizodermis
	B	17.61	Chalcopyrite in siderite	0.21	Magnetite? grain	0.12	Magnetite? grain	0.24	Fe-dendrite on ferrosphere	0.81	Axle roller
	C	0.33	Hematite grain	2.44	Fe-oxide on ferrosphere	0.12	Al-Si-Fe crassinetwork	0.73	Ca-Mg-Fe-Mn carbonate	0.49	Primary cortex
Zn	A	0.50	Vitrinite with siderite	0.11	Teniusphere with Fe-oxide	0.60	Cenosphere	0.16	Magnetite in cenosphere	<0.01	No data
	B	0.72	Pyrite in siderite	0.07	Si microsphere	0.01	No data	0.31	Fusinoid	<0.01	No data
	C	0.84	Siderite grain	1.23	Cenosphere	0.17	Al-Si-Fe crassinetwork	0.46	Hematite in organic	<0.01	No data
As	A	0.41	Fusinite with siderite	0.17	Crassisphere wit Fe-oxide	0.29	Fe-oxide on microsphere	0.58	Fe-oxide in cenosphere	<0.01	No data
	B	0.12	Chalcopyrite in siderite	0.04	Cenosphere	0.22	Calcimagnesiaferrosphere	0.17	Ferrosphere	0.14	Rhizodermis
	C	0.19	Magnetite massive grain	<0.01	No data	0.39	Al-Si-Fe crassinetwork	0.52	Ca-Fe aluminosilicate	<0.01	No data

Table 3. *Cont.*

Element	Area	Feed Coal		Fly Ash		Slag		Topsoil		Root	
		Cn **	Compound	Cn	Compound	Cn	Compound	Cn	Compound	Cn	Compound
Ag	A	0.26	Cassiterite with maceral	0.22	Fe-oxide on Si-microsphere	0.28	Fe-oxide in cenosphere	0.19	Quartz with organic	0.22	Cortex cell
	B	0.19	Hematite with siderite	0.12	Magnetite? on microsphere	0.10	Si-Ca microsphere	0.28	Ferrosphere	0.11	Axle roller
	C	0.65	Fusinite with siderite	0.52	Fe-oxide in cenosphere	0.60	Crassinetwork with Fe-oxide	2.31	Monazite	0.04	Primary cortex
Cd	A	0.35	Cassiterite	0.14	Fe-oxide on cenosphere	0.21	Fe-oxide in cenosphere	0.12	Fe-oxide on Si-cenosphere	0.42	Rhizodermis
	B	0.29	Hematite with siderite	0.23	Cenosphere	0.18	Crassinetwork	0.24	Barite	0.21	Primary cortex
	C	0.61	Siderite grain	0.39	Fe-oxide in cenosphere	0.44	Crassinetwork with Fe-oxide	1.21	Monazite	0.37	Primary cortex
Sb	A	0.53	Vitrinite with siderite	0.24	Fe-oxide on microsphere	0.36	Fe-oxide in cenosphere	0.78	Organic matter	0.62	Primary cortex
	B	0.34	Siderite	0.43	Magnetite? on microsphere	0.29	Ferrosphere	0.22	Cenosphere with Fe-oxide	1.28	Axle roller
	C	0.37	Fusinite with minerals?	0.42	Fe-oxide in cenosphere	0.28	Al-Si-Fe crassinetwork	1.20	Ca-Mg-Fe-Mn carbonate	0.52	Rhizodermis
Pb	A	2.86	Cassiterite with maceral	1.37	Fe-oxide on cenosphere	1.72	Fe-oxide on microsphere	1.47	Cenosphere	1.16	Primary cortex
	B	1.62	Hematite with siderite	0.68	Cenosphere	0.69	Cenosphere	1.02	Siderite after hematite	0.63	Axle roller
	C	3.79	Siderite grain	1.07	Fe-oxide on crassinetwork	0.47	Crassinetwork with Fe-oxide	1.60	Siderite after hematite	0.80	Primary cortex

* The name and location of the tested area is as given in Figure 1. ** Cn—content (in wt %); detection limit = 0.01%.

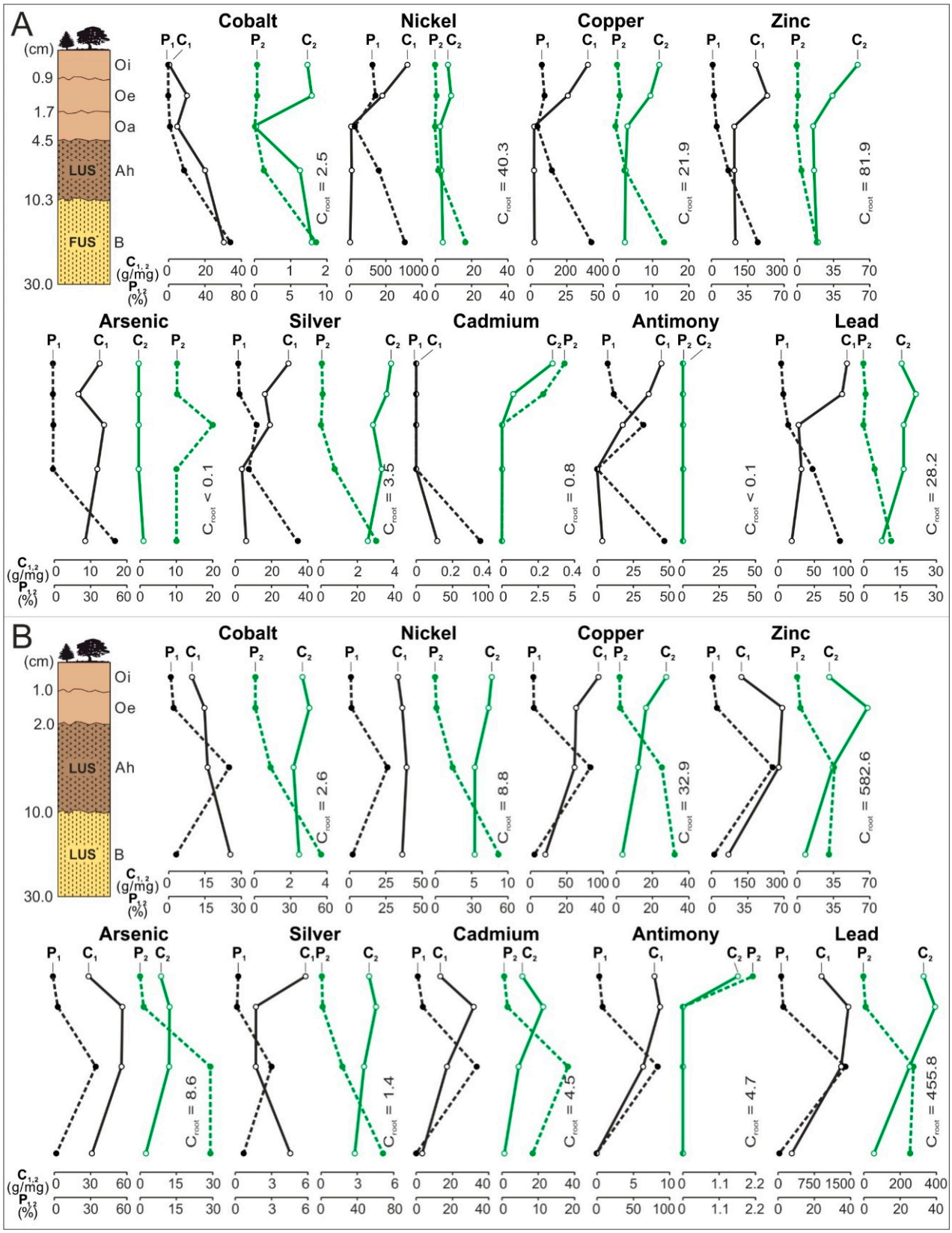

Figure 3. *Cont*.

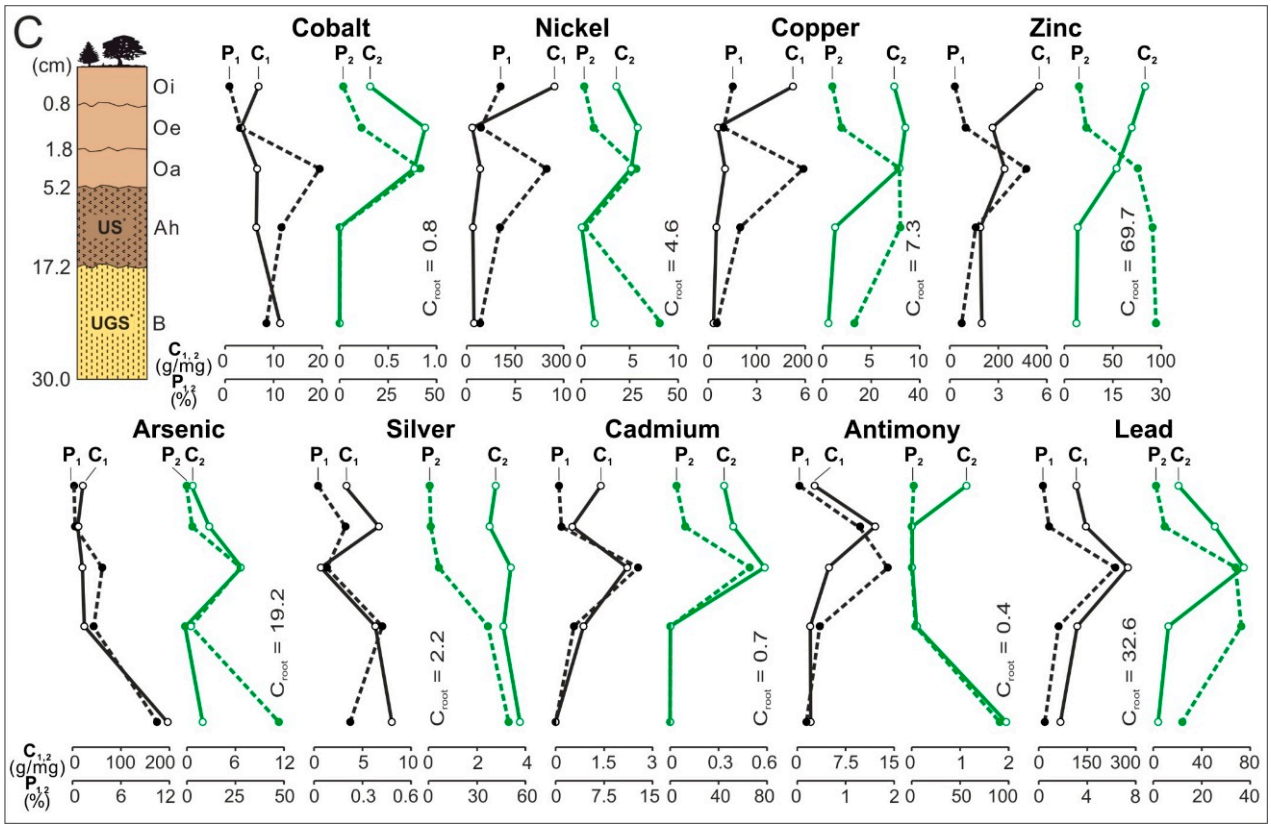

Figure 3. The content of elements in magnetic (C_1) and nonmagnetic fractions (C_2) and their proportions in determining the average element concentration in the whole subhorizon/horizon of the topsoil (respectively, P_1 and P_2), and also the element content in tree roots and undergrowth (C_{root}) in topsoil in the tested areas (**A**–**C**). * Soil granulometric groups: LUS—loamy and unsorted sand, FUS—fine and unsorted sand, US—unsorted sand, UGS—unsorted and gravelly sand.

Fine roots of Scots pines, common oaks, and the undergrowth found in the top layer of the soil in areas A–C, generally have higher content of Ni, Cu, As, Cd, and Pb than the roots of trees of the *Pinaceae* (*Pinaceae* Lindl.) and the roots of the trees discussed by other authors [38,111]. The content of Co, Zn, Ag, and Sb in the analyzed roots is hard to assess due to lack of the comparative data (Table 2).

3.2. Distribution and Mode of Occurrence of the Elements in Coal and Combustion Residues

Feed coal. Feed coalfrom power stations differs in its petrographic and chemical composition although it comes from the same Upper Silesian Coal Basin (Tables 1 and 2). Moreover, the feed coals are characterized by an individual for each power plant's (PS-a, PS-b, and PS-c) collection of minerals and macerals with the maximum content of elements (Table 3, see Table S3). Based on the literature and the current understanding, it may be concluded that it is an expected tendency. The often described variability of coal quality within a coal basin, a coal deposit and a coal seam, in Poland (e.g., [83,113–115]), and around the world (vast literature, (e.g., [5,8,9,116]), together with the methods of purification and carbonization of feed coal, commonly applied in PS, make it impossible to expect constant petrographic and chemical properties of the feed coal. It is assumed that the content and probably also the mode of occurrence of the trace elements in coal is different before and after coal cleaning of the mineral matter interlayers (e.g., [117–121]). It is supposed that the mode of EE occurrence in the feed coal from the Upper Silesian and Lublin Coal Basin is an individual property of each feed coal and it may differ from the hitherto determined mode of occurrence of the elements in raw coal [20].

Based on the results presented in Section 3.2. (see Figure 2, Table S1) it may be noticed that the minerals in the magnetic fraction play a crucial role in concentrating the

analyzed elements in feed coal. Although the highest episodic content of the elements was observed in iron and tin oxides (concerning Co, Ni, Cu, As, Ag, Cd, Pb), in the intergrowths of macerals with siderite (Co, Zn, As, Ag, Cd, Sb, Pb) and in sulfides (Cu, Zn, and As; Table 3, see Table S3) yet the hosts of the elements are, most often,(except magnetite/hematite) fusinite (mainly with inclusions of pyrite, carbonate sand clay minerals), pyrite and chalcopyrite, followed by siderite, vitrinite (often with minerals), and dolomite. The observations confirm and complement the hitherto observed regularities concerning the role of pyrite, native sulfides of the elements, carbonate minerals and clay minerals in concentrating the analyzed elements (vast literature, e.g., [5,8,122–127]). It is assumed that elements, most often chalcophilous ones, isomorphically replace Fe and/or S in pyrite, and Fe, Mn, Mg, and Ca can replace one another in carbonates (e.g., [128–130]). Additionally, nanoparticles of sulfides and sulfosalts containing e.g., Co, Cu, Ni, Pb, and Zn, may grow into grains of other minerals, which is often observed in the minerals of hydrothermal origin (e.g., [131–133]). Probably, the isomorphic admixtures of Co, Ni, Cu, Zn, As, Cd, Sb, and Pb, which were identified in the analyzed magnetite/hematite and cassiterite (Table 3, Figure 4),are usually found in various magmatic and hydrothermal ore-forming environments [134–136].It is generally believed that the minerals are the hosts of the highest content and the highest number of trace elements in coal [9]. Probably, some of the elements were also absorbed by the organic matter and are included in the structure of macerals in nonmineral bindings, in form of compounds similar to organic compounds. It is assumed that the latter forms consist of the elements adsorbed on the surface of organic substances, the elements dissolved in water in pores, and the elements bound in submicro- or nanomicrominerals, surrounded by the organic matter of coal [11].It is probable that such forms of occurrence of Co, Ni, Cu, Zn, As, Ag, Cd, Sb, and Pb in the organic matter (see Table S3), with constantly high yields of the matter in the analyzed feed coal (Table 1) make the nonmagnetic fraction of the feed coal (including organic matter) determine the average content of the elements in the whole feed coal (Figure 2, see Table S1).

Combustion residues. Among the analyzed components of the residue remaining after combusting the feed coal, the highest content of the elements is observed in the <0.05 mm magnetic fraction of the fly ash (mainly from PS-a and PS-b), and sporadically in the >0.5 mm and 0.05–0.2 mm magnetic particles (Figure 2, see Table S1). The highest content of the elements in the slag was also observed in the magnetic fraction. The observations confirm and expand the understanding of the hitherto observed regularity i.e., more intensive condensation of most EE on fine particles of the fly ash than on the particles of the slag and the bottom ash (vast literature, e.g., [16,22–24,137]). According to Wang et al. [138] the described tendency results from the higher surface activity and the ability to absorb elements on small surfaces, than on thick particles of the fly ash. The SEM/EDS analysis showed that microspheres and ferrospheres incrusted with crystals, dendrites and/or iron oxides, single grains of magnetite (concerns Co, Ni, Cu, Ag, Cd, Sb, and Pb), as well as tenui- and crassispheres, and cenospheres with grains of magnetite (concerns Zn and As; Table 3, see Table S3, Figure 4) are the hosts of the highest content of elements in the fly ash. In turn, the hosts of the highest content of the elements in the slag are iron oxides on the surface of cenospheres, crassinetwork, ferrospheres, and iron oxide grains, and more seldom apatite. The biggest influence on the average content of the elements in the whole fly ash and the whole slag has a group of particles of the greatest yield and, simultaneously, relatively high content of the elements, that is mainly the <0.05 mm nonmagnetic particles of the fly ash and the nonmagnetic fraction of the slag. The aforementioned forms of the fly ash and the slag particles supplement the vast range of residue forms remaining after combusting the feed coal with trace elements, rare elements and radioactive elements, already presented by many authors (e.g., [21,25,28,109,139–146]).

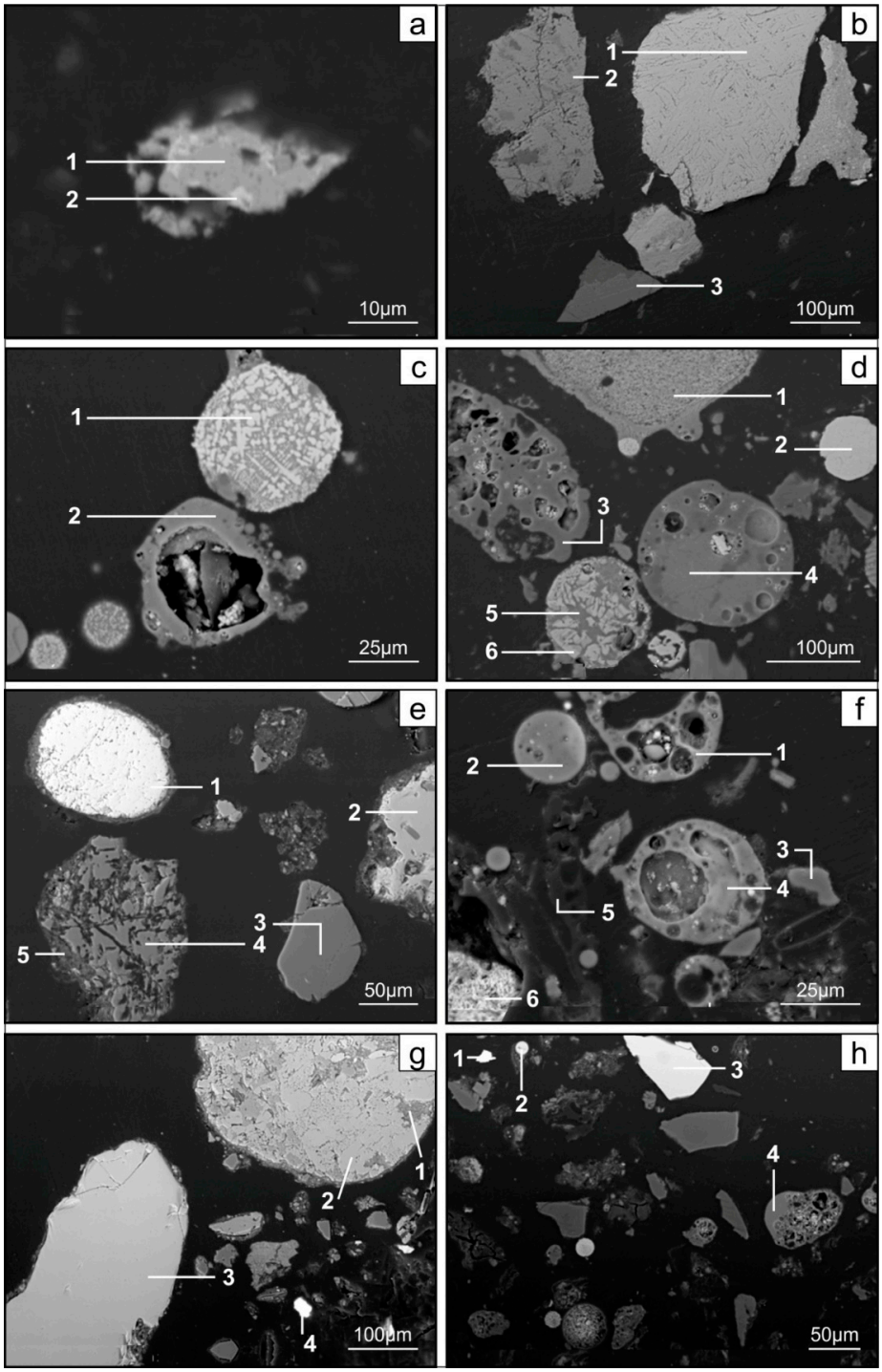

Figure 4. *Cont*.

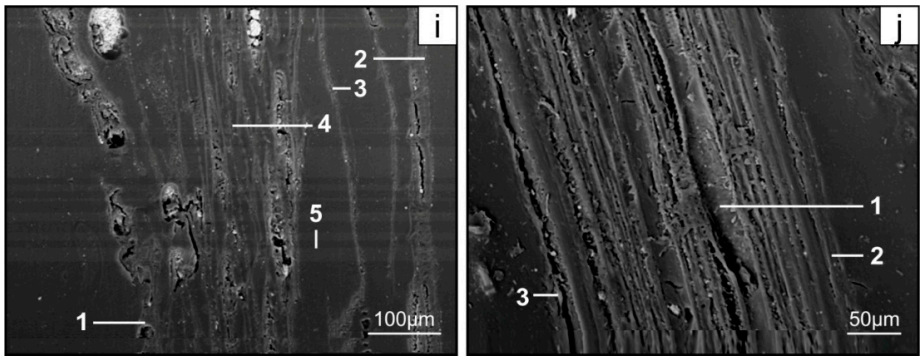

Spectrum (photo)	Analysis Point	Element Contents (wt %)									
		Co	Ni	Cu	Zn	As	Ag	Cd	Sn	Sb	Pb
a	1	Nd *	0.10	nd	nd	0.16	Nd	0.35	75.43	nd	1.57
	2	0.01	0.17	1.51	0.06	nd	0.26	nd	57.34	nd	2.86
b	1	nd	0.16	nd	nd	nd	0.01	0.03	nd	nd	nd
	2	0.03	0.25	0.31	nd	0.09	Nd	0.11	nd	0.04	nd
	3	nd	0.15	nd	nd	nd	Nd	0.19	nd	0.22	0.75
c	1	nd	0.34	nd	nd	nd	Nd	0.05	nd	0.07	nd
	2	nd	0.16	nd	nd	nd	Nd	0.14	nd	nd	nd
d	1	nd	nd	nd	nd	nd	Nd	0.13	nd	nd	nd
	2	nd	nd	nd	nd	nd	Nd	0.13	nd	0.1	0.24
	3	0.07	0.04	0.06	nd	nd	Nd	nd	nd	0.03	0.69
	4	0.10	0.04	nd	nd	nd	Nd	nd	nd	nd	nd
	5	nd	0.07	nd	nd	nd	Nd	0.14	nd	nd	0.04
	6	0.03	nd	0.03	nd	nd	Nd	nd	nd	0.16	nd
e	1	nd	0.01	0.01	0.07	nd	0.06	nd	nd	0.05	nd
	2	0.04	0.07	nd	nd	0.11	0.06	nd	nd	nd	nd
	3	0.01	nd	nd	nd	nd	0.19	nd	nd	nd	0.80
	4	nd	0.05	0.01	nd	nd	Nd	nd	nd	nd	0.05
	5	nd	0.06	nd	nd	nd	Nd	0.05	nd	0.02	0.23
f	1	0.07	0.10	nd	nd	nd	Nd	nd	nd	nd	0.33
	2	0.03	0.03	0.15	nd	nd	Nd	nd	nd	nd	0.43
	3	nd	0.03	nd	nd	nd	Nd	nd	nd	0.11	nd
	4	0.02	0.01	0.05	0.02	nd	Nd	nd	nd	0.10	nd
	5	0.06	0.06	0.06	nd	nd	0.01	nd	nd	0.15	nd
	6	nd	0.03	nd	nd	nd	Nd	nd	nd	0.11	nd
g	1	0.10	nd	0.06	nd	nd	Nd	nd	nd	nd	nd
	2	nd	0.08	0.04	nd	nd	Nd	nd	nd	nd	0.32
	3	0.03	nd	0.17	nd	nd	Nd	0.14	nd	0.12	nd
	4 **	nd	nd	nd	nd	nd	2.31	1.25	nd	nd	0.20
h	1 ***	0.20	0.39	0.01	0.07	nd	Nd	nd	nd	nd	nd
	2	0.27	nd	0.07	nd	0.15	Nd	nd	nd	nd	nd
	3	nd	0.20	nd	nd	nd	Nd	0.02	nd	0.14	nd
	4	nd	0.22	nd	nd	nd	Nd	nd	nd	nd	nd
i	1	nd	0.30	0.02	nd	nd	0.11	nd	nd	nd	nd
	2	0.17	nd	nd	nd	nd	Nd	0.05	nd	nd	nd
	3	nd	0.26	nd	nd	nd	Nd	0.10	nd	nd	0.04
	4	0.13	0.36	nd	nd	nd	Nd	0.20	nd	0.12	0.29
	5	nd	0.21	nd	nd	nd	Nd	nd	nd	0.18	0.57
j	1	0.01	0.10	0.21	nd	nd	Nd	0.11	nd	0.12	nd
	2	nd	0.14	0.02	nd	nd	Nd	0.09	nd	0.04	nd
	3	0.14	0.22	0.33	nd	nd	Nd	nd	nd	0.52	nd

Figure 4. SEM/EDS trace element analysis (wt%) done on cross sections of the feed coal, fly ash, slag, topsoil, and root samples. (**a**) feed coal from PS-a: 1—cassiterite, 2—cassiterite with element inclusion, (**b**) feed coal from PS-c: 1—magnetite, 2—hematite, 3—Mg-siderite, (**c**) magnetic fraction of the fly ash >0.5 mm from PS-a: 1— magnetite dendrite on cenosphere, 2—plerosphere, (**d**) magnetic fraction of the slag from PS-b: 1—Fe-peryclase, 2—ferrosphere, 3—cenosphere, 4—cenosphere with magnetite inclusions, 5—Ca-Mg-ferrosphere, 6—magnetite on the Ca-Mg-ferrosphere, (**e**) magnetic fraction of the soil horizon B in area A: 1—magnetite sphere, 3—quartz with organic inclusion, 4—feldspar, 5—feldspar with organic inclusion,

*

(**f**) magnetic fraction of the soil horizon Ah in area B: 1—wall of cenosphere, 2—cenosphere, 3—quartz, 4—cenosphere, 5—crassisphere with small cenosphere, 6—quartz with Fe dendrite, (**g**) magnetic fraction of the soil horizon B in area C: 1—K-feldspar, 2—plagioclase, 3—Fe-aluminosilicate, 4—monazite, (**h**) magnetic fraction of the soil horizon Ah/B in area B: 1—barite, 2—ferrosphere, 3—sharp-angled grain of magnetite, 4—cenosphere with Fe-oxide particles, (**i**) root from topsoil in area A: 1—rhizodermis, 2—the cell wall of the primary cortex, 3—axle roller, 4—the interior of the primary cortex cell, 5—rhizodermis, (**j**) root from topsoil in area C: 1—axle roller, 2—rhizodermis, 3—rhizodermis. * nd—no data. also identified: ** La = 6.15 %. Ce = 230.35 %. Pr = 3.95 %. Nd = 9.32 %; *** Ba = 0.56.

The distribution of the elements in the fly ash and the slag probably results from the mode of occurrence of the elements in the organic and mineral matter of the feed coal. Based on the results of research obtained by other authors [12–15,17–19,147], it may be expected that the analyzed elements (Co, Ni, Cu, Zn, As, Ag, Cd, Sb, and Pb) occurring in macerals and pyrite, as well as Ni, Cu and As observed in chalcopyrite (Table 3, see Table S3), were the first ones to evaporate in the furnaces of the discussed PS. Due to the temperature of evaporation of the elements [148], this could occur in such an order: Cd, Pb, Zn, Sb, As, Cu, Ni, and Co. The volatility of the elements is variable, i.e., different at the initial stage of coal combustion in a power station, and different during the main stage of combustion [2,3,149–151]. It is probable that most of the vapors of the analyzed elements condensed on the surface of microspheres and unburnt organic matter; then they crystallized in forms showed in Figure 4, i.e., euhedral ferrospinels, dendrites, magnetite, Ti-magnetite, and hematite. The data presented in Table 4 indicate an above-average share of whole not full burned in the concentration of the EE discussed. The organic matter present in the slag hosts Co, Ni, Zn, Cd, and Ag; present in fly ash with a diameter >0.5 mm is an As host, and not full burned organic matter present in the class of particles with a size <0.05 mm is an Sb and Pb host. Such a scenario of coal combustion, hitherto observed in many power stations (vast literature, e.g., [22,141,152]), can cause the observed accumulation of the analyzed elements on the fly ash particles.

Summarizing the discussion in this section, it can be stated that the highest episodic content of the elements was found in iron and tin oxides (concerns Co, Ni, Cu, As, Ag, Cd, Pb), in the intergrowths of macerals with siderite (Co, Zn, As, Ag, Cd, Sb, Pb) and in sulfides (Cu, Zn, and As); the hosts of the elements are, most often, (except magnetite/hematite) fusinite (mainly with inclusions of or fused with pyrite, carbonates and clay minerals), pyrite and chalcopyrite, followed by siderite, vitrinite (often fused with minerals), and dolomite; however, the most significant influence on the average content of elements in whole feed coal is the nonmagnetic fraction of the coal feed (including organic matter). Due to thermal transformations of coal feed in the combustion chamber, the way elements occur in combustion residues is different. Microspheres and ferrospheres incrusted with crystals, dendrites and/or iron oxides, single grains of magnetite (concerns Co, Ni, Cu, Ag, Cd, Sb, and Pb), as well as tenui- and crassispheres, and cenospheres with grains of magnetite (concerns Zn and As) are the hosts of the highest content of elements in the fly ash. In turn, the hosts of the highest content of the elements in the slag are iron oxides on the surface of cenospheres, crassinetwork, ferrospheres, and iron oxide grains, and more seldom apatite; however, the biggest influence on the average content of the elements in the whole fly ash and the whole slag has a mainly the <0.05- mm nonmagnetic particles of the fly ash and the nonmagnetic fraction of the slag.

It seems to be accurate to assume that, if the finest solid particles found in the <0.05 mm fraction of the analyzed fly ash are emitted by the power stations, then they were the particles most enriched with Co and Cu (in areas A–C), Ni, Zn and Pb (A, C), As and Sb (C), and Cd (A) (Figure 5, see Table S4), in comparison with the feed coal, which reached the analyzed topsoil, whereas the >0.5 mm fly ash particles, enriched mainly with As, Ag, and Cd, were probably separated by the electrostatic precipitators.

Table 4. Yield fractions, Fe and unburned organic matter content in magnetic fraction, and element contents in whole not full burned organic matter from magnetic fraction of the fly ash and slag from power stations PS-a, PS-b, and PS-c.

Object/PS/Element	Fly Ash				Slag
	>0.5 mm	0.5–0.2 mm	0.2–0.05 mm	<0.05 mm	
Yield of Magnetic Fraction (wt %)					
PS-a	0.03	1.96	3.98	26.01	15.07
PS-b	0.37	1.85	11.67	6.30	7.84
PS-c	0.11	3.57	6.26	2.39	10.54
Yield of Nonmagnetic Fraction (wt %)					
PS-a	0.08	13.73	22.42	31.79	84.93
PS-b	0.28	8.88	49.58	21.07	92.16
PS-c	0.09	5.99	31.32	50.27	89.16
Fe content in Magnetic Fraction (wt %)					
PS-a	5.30	7.65	15.33	21.60	13.57
PS-b	39.30	12.72	33.47	33.01	7.60
PS-c	4.24	2.66	9.84	14.14	12.61
Content of Unburned Organic Matter in Magnetic Fraction (vol %)					
PS-a	5	4	<0.5	<0.5	1
PS-b	2	6	<0.5	<0.5	<0.5
PS-c	8	3	<0.5	<0.5	4
Element Content in Unburned Organic Matter in Magnetic Fraction (wt %)					
			PS-a		
Co	0.07	no data	no data	0.02	0.11
Ni	<0.01	no data	no data	<0.01	<0.01
Cu	<0.01	no data	no data	<0.01	<0.01
Zn	0.08	no data	no data	<0.01	0.60
As	0.15	no data	no data	<0.01	0.08
Ag	<0.01	no data	no data	<0.01	<0.01
Cd	<0.01	no data	no data	<0.01	<0.01
Sb	<0.01	no data	no data	0.26	0.15
Pb	<0.01	no data	no data	0.52	<0.01
			PS-b		
Co	<0.01	no data	<0.01	<0.01	0.14
Ni	<0.01	no data	0.10	<0.01	0.08
Cu	<0.01	no data	0.16	<0.01	<0.01
Zn	<0.01	no data	<0.01	<0.01	<0.01
As	<0.01	no data	<0.01	<0.01	<0.01
Ag	<0.01	no data	<0.01	<0.01	0,01
Cd	<0.01	no data	<0.01	<0.01	0.14
Sb	<0.01	no data	<0.01	<0.01	<0.01
Pb	0.54	no data	<0.01	<0.01	0.09
			PS-c		
Co	<0.01	0.10	no data	0.02	<0.01
Ni	0.05	0.04	no data	<0.01	0.07
Cu	<0.01	<0.01	no data	<0.01	<0.01
Zn	<0.01	<0.01	no data	<0.01	0.13
As	<0.01	<0.01	no data	<0.01	0.28
Ag	<0.01	<0.01	no data	<0.01	0.60
Cd	<0.01	<0.01	no data	<0.01	0.29
Sb	<0.01	<0.01	no data	0.26	<0.01
Pb	0.12	<0.01	no data	0.53	<0.01

3.3. Distribution and Mode of Occurrence of the Elements in Topsoil and Roots

The results clearly indicate that the magnetic particles of the mineral matter occurring in the organic horizon of soil play a large role in concentrating the analyzed elements (Co, Ni, Cu, Zn, As, Ag, Cd, Sb, and Pb) in the whole topsoil in areas A, B, and C (Figure 3, Table S2). The highest content of the elements was observed in subhorizon Oi (most often) and Oe (secondarily), and even more seldom in horizon B. The hosts of the elements are most often various morphotypes of microspheres and char, more often autochthonic organic matter as well as transformed and/or newlyformed carbonate minerals (Table 3, see Table S3). The morphology of the microspheres and char identified in the topsoil is very similar to the fly ash particles described above (Table 3, see Table S3, Figure 4), emitted by power stations in areas A–C. The observations prove that the particles which are the most common hosts of the elements in the analyzed topsoil are of the anthropogenic origin. The soil samples were collected along the main direction of wind, downwind of the emitters of the particles. The results clearly indicate that combusting coal in the power stations (PS-a, PS-b, and PS-c) is the main cause of why the anthropogenic particles occur in the topsoil and why the content of the discussed elements in the studied areas A–C is heightened in comparison with the reference values (Table 2). Considering the fact that there are no other industrial emitters of pollution in areas A and C, presumably power stations PS-a and PS-c are the only emitters of the elements into the topsoil in these areas. In the statement above, it is assumed that the low emission from home furnaces and the pollution emission from high industrial smokestacks are an irrelevant source of EE (which is not analyzed in the research). In turn, in area B, apart from power station PS-b, there are also other significant emitters of the elements. The sharp-edged grains of magnetite, containing admixtures of the elements, occurring in horizon O and Ah (Figure 4, see Table S3), prove it; such grains of magnetite in the topsoil are considered to be products of ironworks and possibly of nonferrous smelters in area B [153,154].

The dusts emitted by the power stations (PS-a, PS-b, and PS-c) into the atmosphere, of the content of the analyzed elements similar to the content of the elements in the <0.05 mm fly ash particles (see Table S2), are probably a sediment which is highly enriched with the elements. The average enrichment of such a sediment/fly ash with EE is between 1.4, for the magnetic fraction, and 1995.2, for the nonmagnetic fraction (Figure 5). In given power stations, for the <0.05 mm particles, the enrichment factor with the elements is even greater (Table S4). Among the <0.05 mm particles, which are potentially emitted by PS, the magnetic particles (mainly ferrospheres, cenospheres with incrustations of crystals, and dendrites; see Figure 4, Table S3) are enriched with the elements to a similar degree (Ag, Cd, and Pb) or more (Co, Ni, Cu, Zn, As, and Sb), than the nonmagnetic particles. Due to this fact, in the vicinity of the emitters, a significant increase in the magnetic susceptibility and in the content of the elements in the topsoil may be expected. The heightened values of the indices in the vicinity of power stations and metal works are still observed in many countries in the world (vast literature, (e.g., [155–158])).

It was also concluded that the values of the enrichment factor of magnetic fractions of the topsoil with the analyzed elements are always greater than in the nonmagnetic fraction (Figure 5). This results from the aforementioned high content of the elements in the magnetic particles of the dust emitted by PS, and the ability of iron oxides (mainly magnetite) to absorb elements in the soil and the water environment. The abilityis often employed to immobilize EE in soil, sewage, and wastewater [159–161]. It is assumed that the elements (Be, Cd, Co, Cu, Fe, Mg, Mn, Ni, Pb, REE, Si, Sn, Th, Tl, U, and Zn) are more easily leached into an acidic environment than into an alkaline one (vast literature, e.g., [29–31]). Primarily, there were leached the elements from a few-micron-thick outer layer of the particles with a size<0.05 mm emitted by PS-a, PS-b, and PS-c. It is assumed that the elements occurring within particles are leached more slowly because of the limited availability of solutions [162–164]. The leached elements (here: Co, Ni, Cu, Zn, As, Ag, Cd, Sb, Pb) were probably sorbed by the organic matter occurring in horizon O and Ah. It is known that the matter has a strong tendency to absorb heavy metals and form metalorganic compounds with them (e.g., [165,166]), while the deposited dust particles

passed into deeper and deeper topsoil subhorizons together with the deposited organic and mineral matter of mainly nontechnogenic origin.

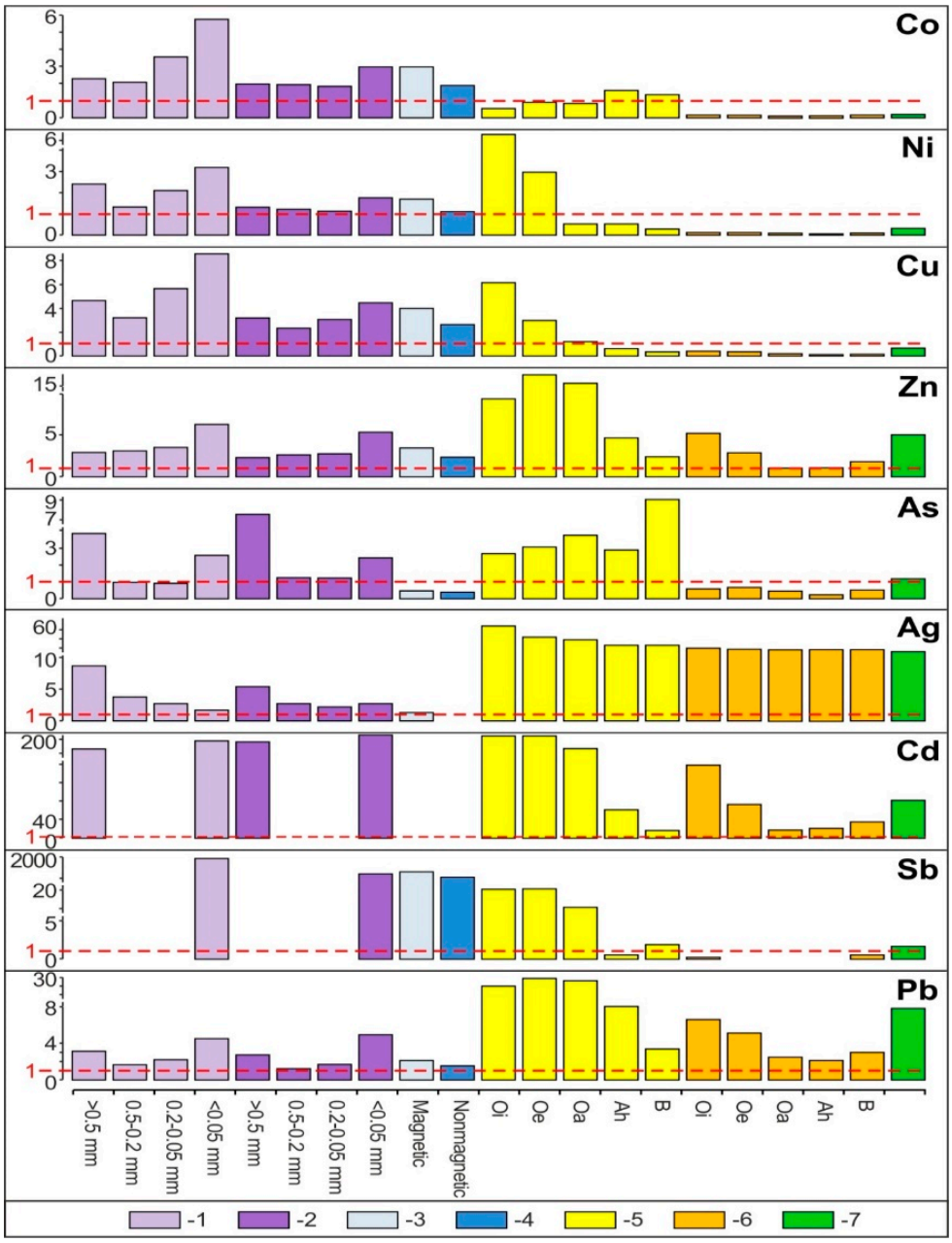

Figure 5. Enrichment factor of the fly ash, slag, topsoil and roots compared to feed coal.Fly ash: 1—magnetic fractions, 2—nonmagnetic fraction; 3 and 4—slag; topsoil: 5—magnetic fraction, 6—nonmagnetic fraction; 7—roots.

It is worth noticing that the content of Zn, As, Cd, and Pb in each subhorizon/horizon of the topsoil in area B is greater thanin the <0.05 mm fly ash particles, potentially emitted into the atmosphere, and greater than in the soil in areas A and C (Figure 5). The observation indicates that, apart from power station PS-b, there are other emitters of the elements into the topsoil. This is exactly the casein area B [167]. The most significantemitters of Zn, As, Cd, and Pb in area B (apart from PS) are home furnaces, and, in the past, also zinc, lead and ironworks. The result is the often-observed high content of EE in the topsoil in the vicinity of the emitters [152,168,169].

The above average content of the elements in the topsoil, in comparison with podzols (Table 2), resulted in a significant increase in the content of the elements in the roots of trees and undergrowth (Figure 3, see Table S2). Among the studied areas, the roots of trees and undergrowth growing in area A have the highest content of Ni and Ag;the roots in area B have the highest content of Co, Cu, Zn, Cd, Sb, and Pb; and the roots in area C have the highest content of As. The enrichment factor shows the depletion of tree roots in Co, Ni, and Cu (EF = 0.2–0.6) and the enrichment in Zn, As, Ag, Cd, Sb, and Pb (EF max = 192.2) compared to the EE content in the coal feeds (Figure 5, Table S4). EF values are generally proportional to the increase in the content of the elements in the topsoil. It is assumed that the high content of EE in soil has a negative influence on the content of the elements in the roots of trees, and, in turn, in the above-ground portion of the plants. It also adversely affects the development and activities of soil microorganisms, their population and species diversity [37–40]. The content and toxicity of the indispensable EE (Zn, Cu, Mn, Fe, Ni, and Co), and the ones irrelevant for plant growth (As, Ag, Cd, Sb, Hg, Tl, Pb), depend on their bioavailability in the soil. The sensitivity of undergrowth and tree species is also important and it affects changes in the properties of soil [39,170]. The SEM/EDS analysis showed that the hosts of the elements in the roots of trees and the undergrowth growing in area A are the primary cortex (for Co, Ni, Sb, and Pb), rhizodermis (Cu and Cd), and cortex cells (Ag). In area B, the hosts are the primary cortex (Co, Ni, and Cd), rhizodermis (As), and axle rollers (Cu, Ag, Sb, and Pb). In area C, the host of Co and Sb is rhizodermis, and the carrier of Ni, Cu, Ag, Cd, and Pb is primary cortex (Figure 4, Table 3).

In this way, the presented work expands onthe previous data concerning the accumulation of the high content of elements in the rootlets [171,172], and the tendency of the elements to concentrate in the outer tissue of the roots, i.e., in the rhizodermis and in the primary cortex (Figure 4, Table 3), which was also noticed by Kidd et al. [173], Antoniadis et al. [174], and Vatanseveret al. [42].

The paper omits the discussion on the behavior of elements in the soil under the influence of aqueous solutions after sedimentation of particles from the power station, and the influence of the soil substrate on the content of elements in the topsoil was also omitted; this was beyond the purpose and scope of this study, but may be developed and published later.

4. Conclusions

1. The hosts of the elements in the feed coal are most often: magnetite, fusinite (mainly with ingrowths or agglomerate with pyrite, carbonates, and clay minerals) together with pyrite and chalcopyrite, followed by siderite, vitrinite (often fused with minerals) and dolomite, present in the magnetic fractions of the feed coal. The highest point of content of the elements was observed in magnetite and cassiterite (Co, Ni, Cu, As, Ag, Cd, Pb), in macerals with siderite (Co, Zn, As, Ag, Cd, Sb, Pb) as well as in pyrite and chalcopyrite (Cu, Zn, and As). The nonmagnetic fraction has the greatest influence on the average content of the elements in the whole feed coal.
2. The hosts of the highest content of the elements in the fly ash are microspheres and ferrospheres incrusted with crystals, dendrites and/or iron oxides (mainly of magnetite), and single grains of magnetite (concerns Co, Ni, Cu, Ag, Cd, Sb, and Pb), as well as tenuispheres and crassispheres, cenospheres, and subhedral grains of magnetite (Zn and As), being the main components of the magnetic fraction of the fly ash and the slag. The hosts of the highest content of theelements in the slag are iron oxide on the surface of cenospheres and the crassinetwork, ferrospheres, and iron oxide grains. More rarely the host is is apatite. The biggest influence onthe average content of the elements in the whole fly ash and the whole slag has a group of <0.05 mm nonmagnetic particles of the fly ash and the nonmagnetic fraction of the slag. If the finest solid particles found in the <0.05 mm fraction of the analyzed fly ash are emitted by the power stations, then they were the particles most enriched with Co and Cu (in areas A–C), Ni, Zn and Pb (A, C), As and Sb (C), and Cd (A), in comparison

with the feed coal, which reached the analyzed topsoil, whereas the >0.5 mm fly ash particles, enriched mainly with As, Ag, and Cd, were probably separated by the electrostatic precipitators.

3. In subhorizon Oi, and secondarily in Oe, the content of theelements is the highest. Most often their hosts are various morphotypes of microspheres and char, emitted by power stations located in large wooded areas (area A and C). The content of Zn, As, Cd, and Pb in each subhorizon/horizon of the topsoil in the area exposed to many years of industrial activities (area B) is greater than in the potentially emitted<0.05 mm particles of the fly ash. It is also greater than in the soil in areas A and C. Together with the power station(PS-b) the main emitters of the elements on the surface of the soil in area B were probably zinc, lead, and ironworks (operating in the past). The values of the enrichment factor for the magnetic fraction of the topsoil are always higher than the for the nonmagnetic fraction. The particles of the topsoil show lower enrichment with Co, Cu, Cd, and Sb and greater enrichment with Ni, Zn, As, Ag, and Pb, than the <0.05 mm particles of the fly ash. The elution of elements accumulated in the several-micron surface layer of sedimenting particles (mainly <0.05 mm), with the use of rainwater or flowing water, can still enrich topsoil with ecotoxic elements.
4. The significant enrichment of the topsoil with the elements resulted in an increase in the content of the elements in the roots of trees and undergrowth. In the soil exposed to the long-term emission of the technogenic particles by thermo-emitters (area B), the roots have the highest content of Cu, Zn, Cd, Sb, and Pb, and in the topsoil in the wooded areas with the power station as the only pollution emitter, the roots had the highest content of As (area C) and Ag (area A). The enrichment of the roots with Ci, Ni, Zn, As, Ag, Sb, and Pb is between 0.2 for Co and 41.0 for Cd. It is usually proportional to the increase in the content of the elements in the whole topsoil and the value of the enrichment factor for the topsoil. The highest content of the elements occurs in the tiny roots, especially in the rhizodermis and the primary cortex, more seldom in the axle roller and cortex cells.
5. Along the way from the feed coal to the roots, the highest enrichment with elements was observed in the <0.05 mm magnetic (for Co, Ni, Cu, Zn, Cd, Sb, and Pb) and nonmagnetic (Cd, Sb, and Pb)particles of the fly ash; in the >0.5 mm nonmagnetic particles of the fly ash (As and Ag); in the magnetic particles of the slag (Sb), and in the magnetic particles of the soil in subhorizon/horizon Oi (Ni, Cu, and Ag), Oe (Zn, Cd, Sb, and Pb), Ah (Co), and in horizon B (As). A high content of elements in particles of falling dust from power plants, which is potentially dangerous for topsoil and plants, can be significantly reduced by preparing coal which is free from extremely high content of ecotoxic elements. The choice of methods for obtaining such coal will be facilitated by studies of the occurrence and distribution of elements in the feed coal.

Supplementary Materials: The following are available online at https://www.mdpi.com/2075-163X/11/2/133/s1, Table S1: Yields of fractions and element contents (ppm, g/Mg) in fractions in the feed coals, fly ash, and slag from the power plants (PS-a, PS-b, and PS-c), Table S2: Profile, depth, and yield of horizons/subhorizons of the topsoil, and also the content of the elements in the soil and share of soil horizon in concentration of the elements in whole topsoil, Table S3: Maximum content (wt %) of elements in feed coal, fly ash, slag, topsoil, and roots from areas A, B, and C obtained by the SEM/EDS method, Table S4: Enrichment factor of elements in the fly ash, slag, and topsoil relative to the feed coal, Table S5: Yield fractions, Fe and unburned organic matter content in magnetic fraction, and carbon and element contents in unburned organic fraction from magnetic fraction of the fly ash and slag from power stations PS-a, PS-b, and PS-c.

Author Contributions: Conceptualization, H.R.P.; XRD and SEM/EDS analysis, L.R.; chemical ICP-ES analysis, H.R.P.; investigation, methodology, and resources, H.R.P.; visualization, H.R.P.; translation of the content into English, L.R.; writing and editing, H.R.P. Both the authors have read and agreed to the published version of the manuscript.

Funding: This research received no external funding.

Institutional Review Board Statement: Not applicable.

Informed Consent Statement: Not applicable.

Data Availability Statement: Data is contained within the article and supplementary material.

Conflicts of Interest: The authors declare no conflict of interest.

References

1. Hower, J.C.; Trimble, A.S.; Eble, C.F. Temporal and spatial variations in fly ash quality. *Fuel Proc. Technol.* **2001**, *73*, 37–58. [CrossRef]
2. Zhang, J.; Han, C.-L.; Xu, Y.-Q. The release of the hazardous elements from coal in the initial stage of combustion process. *Fuel Proc. Technol.* **2003**, *84*, 121–133. [CrossRef]
3. Hower, J.C.; Fu, B.; Dai, S. Geochemical partitioning from pulverized coal to fly ash and bottom ash. *Fuel* **2020**, *279*, 118542. [CrossRef]
4. Dzikuć, M.; Kuryło, P.; Dudziak, R.; Szufa, S.; Dzikuć, M.; Godzisz, K. Selected Aspects of Combustion Optimization of Coal in Power Plants. *Energies* **2020**, *13*, 2208. [CrossRef]
5. Yudovich, Y.E.; Ketris, M.P. *Toxic trace Elements in Coals*; Russian Academy of Sciences: Ekaterinburg, Russia, 2005. (In Russian)
6. Ketris, M.P.; Yudivich, Y.E. Estimations of Clarkes for Carbonaceous biolithes: World avarages for trace element contents in black shales and coals. *Int. J. Coal Geol.* **2009**, *78*, 135. [CrossRef]
7. Ward, C.R. Analysis, origin and significance of mineral matter in coal: An updated review. *Int. J. Coal Geol.* **2016**, *165*, 1–27. [CrossRef]
8. Finkelman, R.B.; Palmer, C.A.; Wang, P. Quantification of the modes of occurrence of 42 elements in coal. *Int. J. Coal Geol.* **2018**, *185*, 138–160. [CrossRef]
9. Finkelman, R.B.; Dai, S.; French, D. The importance of minerals in coal as the hosts of chemical elements: A review. *Int. J. Coal Geol.* **2019**, *212*, 103251. [CrossRef]
10. Dai, S.; Bechtel, A.; Eble, C.F.; Flores, R.M.; French, D.; Graham, I.T.; Hood, M.M.; Hower, J.C.; Korasidis, V.A.; Moore, T.A.; et al. Recognition of peat depositional environments in coal: A review. *Int. J. Coal Geol.* **2020**, *219*, 103383. [CrossRef]
11. Dai, S.; Hower, J.C.; Finkelman, R.B.; Graham, I.T.; French, D.; Ward, C.R.; Eskenazy, G.; Wei, Q.; Zhao, L. Organic associations of non-mineral elements in coal: A review. *Int. J. Coal Geol.* **2020**, *218*, 103347. [CrossRef]
12. Linak, W.P.; Wendt, J.O.L. Toxic metal emissions from incineration: Mechanisms and control. *Prog. Energy Combust. Sci.* **1993**, *19*, 145–185. [CrossRef]
13. Querol, X.; Fernández-Turiel, J.L.; López-Soler, A. Trace elements in coal and their behavior during combustion in a large power station. *Fuel* **1995**, *74*, 331–343. [CrossRef]
14. Huang, Y.; Jin, B.; Zhong, Z.; Xiao, R.; Tang, Z.; Ren, H. Trace elements (Mn, Cr, Pb, Se, Zn, Cd and Hg) in emissions from a pulverized coal boiler. *Fuel Proc. Technol.* **2004**, *286*, 23–32. [CrossRef]
15. Sekine, Y.; Sakajin, K.; Kikuchi, E. Release behavior of trace elements from coal during high-temperature processing. *Powder Technol.* **2008**, *180*, 210–215. [CrossRef]
16. Bhangare, R.C.; Ajmal, P.Y.; Sahu, S.K.; Pandit, G.G.; Puranik, V.D. Distribution of trace elements in coal and combustion residues from five thermal power plants in India. *Int. J. Coal Geol.* **2011**, *86*, 349–356. [CrossRef]
17. Sia, S.G.; Abdullah, W.A. Enrichment of arsenic, lead, and antimony in Balingian coal from Sarawak, Malaysia: Modes of occurrence, origin, and partitioning behaviour during coal combustion. *Int. J. Coal Geol.* **2012**, *101*, 1–15. [CrossRef]
18. Hower, J.C.; Dai, S.; Eskenazy, G. Distribution of uranium and other radionuclides in coal and coal combustion products, with discussion of occurrences of combustion products in Kentucky Power Plants. *Coal Comb. Gasif. Prod.* **2016**, *8*, 44–53.
19. Zhao, S.; Duan, Y.; Li, Y.; Liu, M.; Lu, J.; Ding, Y.; Gu, X.; Tao, J.; Du, M. Emission characteristic and transformation mechanism of hazardous trace elements in a coal-fired power plant. *Fuel* **2018**, *2014*, 597–606. [CrossRef]
20. Parzentny, H.R.; Róg, L. Distribution of some ecotoxic elements in fuel and solid combustion residues in Poland. *Energies* **2020**, *13*, 1131. [CrossRef]
21. Vassilev, S.V.; Vassileva, C.G.; Karayigit, A.I.; Bulut, Y.; Alastuey, A.; Querol, X. Phase-mineral and chemical composition of composite samples from feed coals, bottom ashes and fly ashes at the Soma power station, Turkey. *Int. J. Coal Geol.* **2005**, *61*, 35–63. [CrossRef]
22. Vejahati, F.; Xu, Z.; Gupta, R. Trace elements in coal: Associations with coal and mineralsmand their behaviour during coal utilization - A review. *Int. J. Coal Geol.* **2010**, *14*, 904–911. [CrossRef]
23. Dai, S.; Zhao, L.; Peng, S.; Chou, C.-L.; Wang, X.; Zhang, Y.; Li, D.; Sun, Y. Abundances and distribution of minerals and elements in high-alumina coal fly ash from the Jungar Power Plant, Inner Mongolia, China. *Int. J. Coal Geol.* **2010**, *81*, 320–332. [CrossRef]
24. Konieczyński, J.; Zajusz-Zubek, E. Distribution of selected trace elements in dust containment and flue gas desulphurisation products from coal-fired Power plants. *Arch. Environ. Prot.* **2011**, *37*, 3–14.

25. Dai, S.; Seredin, V.V.; Ward, C.R.; Jiang, J.; Hower, J.C.; Song, X.; Jiang, Y.; Wang, X.; Gornostaeva, T.; Li, X.; et al. Composition and modes of occurrence of minerals and elements in coal combustion products derived from high-Ge coals. *Int. J. Coal Geol.* **2014**, *121*, 79–97. [CrossRef]
26. Adamczyk, Z.; Komorek, J.; Lewandowska, M. The high temperature ashes (HTA) from bituminous coal combustion as a potential resource of rare carth elements. *Gospod. Sur. Miner. Miner. Resour. Manag.* **2018**, *34*, 135–150.
27. Oetari, P.S.; Hadi, S.P.; Huboyo, H.S. Trace elements in fine and coarse particles emitted from coal-fired power plants with different air pollution control systems. *J. Environ. Manag.* **2019**, *250*, 109497. [CrossRef]
28. Wilczyńska-Michalik, W.; Dańko, J.; Michalik, M. Characteristics of particulate matter emitted from a coal-fired power plant. *Pol. J. Environ. Sud.* **2020**, *29*, 1411–1420. [CrossRef]
29. Izquierdo, M.; Querol, X. Leaching behaviour of elements from coal combustion fly ash: An overview. *Int. J. Coal Geol.* **2012**, *94*, 54–66. [CrossRef]
30. Singh, R.K.; Gupta, N.C.; Guha, B.K. pH dependence leaching characteristics of selected metals from coal ash and its impact on ground water quality. *Int. J. Chem. Environ. Eng.* **2014**, *5*, 218–222.
31. Silva, E.B.; Li, S.; Oliveira, L.M.; Gress, J.; Dong, X.; Wilkie, A.C.; Townsend, T.; Ma, L.Q. Metal leachability from coal combustion residues under different pHs and liquid/solid ratios. *J. Hazard. Mater.* **2018**, *341*, 66–74. [CrossRef]
32. Tian, Q.; Guo, B.; Nakama, S.; Sasaki, K. Distributions and Leaching Behaviors of toxic elements in fly ash. *ACS Omega* **2018**, *3*, 13055–13064. [CrossRef] [PubMed]
33. Zhao, L.; Dai, S.; Finkelman, R.B.; French, D.; Graham, I.T.; Yang, Y.; Li, J.; Yang, P. Leaching behavior of trace elements from fly ashes of five Chinese coal power plants. *Int. J. Coal Geol.* **2020**, *219*, 103381. [CrossRef]
34. Querol, X.; Juan, R.; Lopez-Soler, A.; Fernandez-Turiel, J.L.; Ruiz, C.R. Mobility of trace elements from coal and combustion wastes. *Fuel* **1996**, *75*, 821–838. [CrossRef]
35. Leyval, C.; Turnau, K.; Haselwandter, K. Effect of heavy metal pollution on mycorrhizal colonization and function: Physiological, ecological aspects. *Mycorrhiza* **1997**, *7*, 139–153. [CrossRef]
36. Jamnická, G.; Bučinová, K.; Havranová, I.; Urban, A. Current state of mineral nutrition and risk elements in a beech ecosystem situated near the aluminium smelter in ŽiarnadHronom, Central Slovakia. *For. Ecol. Manag.* **2007**, *248*, 26–35. [CrossRef]
37. Siwek, M. Plants in postindustrial sites, contaminated with heavy metals. Part, I. Uptake, transport and toxicity of heavy (trace) metals. *Wiad. Botan.* **2008**, *52*, 7–22. (In Polish)
38. Kabata-Pendias, A. *Trace Elements of Soils and Plants*, 4th ed.; CRC Press: Boca Raton, FL, USA; Taylor & Francis Group: Abingdon, UK, 2011; p. 534.
39. Luo, X.; Bing, H.; Luo, Z.; Wang, Y.; Jin, L. Impacts of atmospheric particulate matter pollution on environmental biogeochemistry of trace metals in soil-plant system: A review. *Environ. Pollut.* **2019**, *255*, 113138. [CrossRef]
40. Saikia, B.K.; Hower, J.C.; Hood, M.M.; Baruach, R.; Dekaboruah, H.P.; Boruah, R.; Sharma, A.; Baruah, B.P. Petrological and biological studies on some fly and bottom ashes collected at different times from an Indian coal-based captive power plant. *Fuel* **2015**, *158*, 572–581. [CrossRef]
41. Khalid, S.; Shahid, M.; Niazi, N.K.; Rafiq, M.; Bakhat, H.F.; Imran, M.; Abbas, T.; Bibi, I.; Dumat, C. Arsenic Behaviour in Soil-Plant System: Biogeochemical Reactions and Chemical Speciation Influences. In *Enhancing Cleanup of Environmental Pollutants*; Anjum, N., Gill, S., Tuteja, N., Eds.; Springer: Cham, Switzerland, 2017; pp. 97–140.
42. Vatansever, R.; Ozyigit, I.I.; Filiz, E. Essential and Beneficial Trace Elements in Plants, and Their Transport in Roots: A Review. *Appl. Biochem. Biotechnol.* **2017**, *181*, 464–482. [CrossRef]
43. Taylor, M.P.; Mold, S.A.; Kristensen, L.J.; Rouillon, M. Environmental arsenic, cadmium and lead dust emissions from metal mine operations: Implications for environmental management, monitoring and human health. *Environ. Res.* **2014**, *135*, 296–303. [CrossRef]
44. Yang, J.S.; Yang, F.L.; Yang, Y.; Xing, G.L.; Deng, C.P.; Shen, Y.T.; Luo, L.Q.; Li, B.Z.; Yuan, H.L. A proposal of "core enzyme" bioindicator in long-term Pb-Zn ore pollution areas based on topsoil property analysis. *Environ. Pollut.* **2016**, *213*, 760–769. [CrossRef] [PubMed]
45. Xue, S.; Shi, L.; Wu, C.; Wu, H.; Qin, Y.; Pan, W.; Hartkeya, W.; Ciu, M. Cadmium, lead, and arsenic contamination in paddy soils of a mining area and their exposure effects on human HEPG2 and keratinocyte cell-lines. *Environ. Res.* **2017**, *156*, 23–30. [CrossRef] [PubMed]
46. Jasminka, A.; Robert, Š. Distribution of chemical elements in an old metallurgical area, Zenica (Bosnia and Herzegovina). *Geoderma* **2011**, *162*, 71–85. [CrossRef]
47. Li, Y.; Zhang, B.; Liu, Z.; Wang, S.; Yao, J.; Borthwick, A.G.L. Vanadium contamination and associated health risk of farmland soil near smelters throughout China. *Environ. Pollut.* **2020**, *263*, 114540. [CrossRef] [PubMed]
48. Cabała, J.; Warchulski, R.; Rozmus, D.; Środek, D.; Szełęg, E. Pb-Rich Slags, Minerals, and Pollution Resulted from a Medieval Ag-Pb Smelting and Mining Operation in the Silesian-Cracovian Region (Southern Poland). *Minerals* **2020**, *10*, 28. [CrossRef]
49. Kumar, S.; Zhao, M.; Zhang, H.; Rahman, M.A.; Luo, C.; Rahman, M.M. Distribution, contamination status and source of trace elements in the soil around brick kilns. *Chemosphere* **2021**, *263*, 127882. [CrossRef] [PubMed]
50. Cao, L.C.; Lin, C.; Gao, Y.; Sun, C.; Xu, L.; Zheng, L.; Zhang, Z. Health risk assessment of trace elements exposure through the soil-plant (maize)-human contamination pathway near a petrochemical industry complex, Northeast China. *Environ. Pollut.* **2020**, *263*, 114414. [CrossRef]

51. Kowalska, J.; Mazurek, R.; Gąsiorek, M.; Setlak, M.; Zaleski, T.; Waroszewski, J. Soil pollution indices conditioned by medieval metallurgical activity—A case study from Krakow (Poland). *Environ. Pollut.* **2016**, *218*, 1023–1036. [CrossRef]
52. Tume, P.; Barrueto, K.; Olguin, M.; Torres, J.; Cifuentes, J.; Ferraro, F.X.; Roca, N.; Bech, J.; Cornejo, O. The influence of the industrial area on the pollution outside its borders: A case study from Quintero and Puchuncavi district, Chile. *Environ. Geochemi. Health* **2019**, *42*, 2557–2572. [CrossRef]
53. Askari, M.S.; Alamdari, P.; Chahardoli, S.; Afshari, A. Quantification of heavy metal pollution for environmental assessment of soil condition. *Environ. Monit. Assess.* **2020**, *192*, 162. [CrossRef]
54. Bourliva, A.; Papadopoulou, L.; Aidona, E.; Giouri, K.; Simeonidis, K.; Vourlias, G. Characterization and geochemistry of technogenic magnetic particles (TMPs) in contaminated industrial soils: Assessing health risk via ingestion. *Geoderma* **2017**, *295*, 86–97. [CrossRef]
55. Szuszkiewicz, M.M.; Łukasik, A.; Magiera, T.; Szuszkiewicz, M. Technogenic magnetic particles of topsoil from different sources of emission—A case study from upper silesian conurbation, Poland. *MATEC Web Conf.* **2018**, *247*, 00051. [CrossRef]
56. Wilczyńska-Michalik, W.; Michalik, J.M.; Kapusta, C.; Michalik, M. Airborne magnetic technoparticles in soils as a record of anthropocene. *Atmosphere* **2020**, *11*, 44. [CrossRef]
57. Kabala, C.; Galka, B.; Jezierski, P. Assessment and monitoring of soil and plant contamination with trace elements around Europe's largest copper ore tailings impoundment. *Sci. Total Environ.* **2020**, *738*, 139918. [CrossRef]
58. Vaněk, A.; Grösslová, Z.; Mihaljevič, M.; Ettler, V.; Trubač, J.; Chrastný, V.; Penížek, V.; Teper, L.; Cabała, J.; Voegelin, A.; et al. Thallium isotopes in metallurgical wastes/contaminated soils: A novel tool to trace metal source and behavior. *J. Hazardous Mat.* **2018**, *343*, 78–85. [CrossRef]
59. Rahmonov, O.; Krzysztofik, R.; Środek, D.; Smolarek-Lach, J. Vegetation- and environmental changes on nonreclaimed spoil heaps in Southern Poland. *Biology* **2020**, *9*, 164. [CrossRef]
60. Gür, F.; Yaprak, G. Natural radionuclide emission from coal-fired power plants in the southwestern of Turkey and the population exposure to external radiation in their vicinity. *J. Environ. Sci. Health A* **2010**, *45*, 1900–1908. [CrossRef]
61. Vaněk, A.; Grösslová, Z.; Mihaljevič, M.; Trubač, J.; Ettler, V.; Teper, L.; Cabała, J.; Rohovec, J.; Zádorová, T.; Penižek, V.; et al. Isotopic Tracing of Thallium Contamination in Soils Affected by Emissions from Coal-Fired Power Plants. *Environ. Sci. Techn.* **2016**, *50*, 9864–9871. [CrossRef]
62. Turhan, S.; Garad, A.M.K.; Hançerlioğulları, A.; Kurnaz, A.; Gören, E.; Duran, C.; Karataşlı, M.; Altıkulaç, A.; Savacı, G.; Aydın, A. Ecological assessment of heavy metals in soil around a coal-fired thermal power plant in Turkey. *Environ. Earth Sci.* **2020**, *79*, 134. [CrossRef]
63. Sengupta, S.; Chatterjee, T.; Ghosh, P.B.; Saha, T. Heavy metal accumulation in agricultural soils around a coal fired thermal power plant (Farakka) in India. *J. Environ. Sci. Eng.* **2010**, *52*, 299–306.
64. Iruretagoiena, A.R.; Vallejuelo, S.F.O.; Gredilla, A.; Ramos, C.G.; Oliveira, M.L.S.; Arana, G.; Diego, A.; Madariaga, J.M.; Silva, L.F.O. Fate of hazardous elements in agricultural soils surrounding a coal power plant complex from Santa Catarina (Brasil). *Sci. Total. Environ.* **2015**, *508*, 374–382. [CrossRef] [PubMed]
65. Huang, X.; Hu, J.; Qin, F.; Quan, W.; Cao, R.; Fan, M.; Wu, X. Heavy metal pollution and ecological assessment around the Jinsha coal-fired power plant (China). *Int. J. Environ. Res. Public Health* **2017**, *14*, 1589. [CrossRef] [PubMed]
66. Kovalchuk, O.P.; Snitynskyy, V.V.; Shkumbatyuk, R.S. Monitoring of heavy metals content in soils of the areas surrounding Dobrotvir Thermal Power Plant. *Sci. Bull. UNFU* **2017**, *27*, 87–90. [CrossRef]
67. Liu, D.; Quan, Y.; Ren, Z.; Wu, G. Assessment of heavy metal contamination in soil associated with Chinese coal-fired power plants: A case study in Xilingol, Inner Mongolia. *Int. J. Sustain. Dev. World Ecol.* **2017**, *24*, 439–443. [CrossRef]
68. Jankiewicz, B.; Adamczyk, D. Assessing heavy metal content in soils surrounding a power plant. *Pol. J. Environ. Stud.* **2010**, *19*, 849–853.
69. Clark, J.H.A.; Tredoux, M.; van Huyssteen, C. Heavy metals in the soils of Bloemfontein, South Africa: Concentration levels and possible sources. *Environ. Monit. Assess.* **2015**, *187*, 439–452. [CrossRef]
70. Gune, M.M.; Harshavardhana, B.G.; Ma, W.-L.; Balakrishna, K.; Udayashankar, H.N.; Zhang, Z.; Li, Y.-F. Seasonal Variations of Heavy Metals in the Soil Around a Coal-Fired Thermal Power Plant, South-West Coast of India. *Bull. Environ. Contam. Tox.* **2020**, *104*, 602–608. [CrossRef]
71. Zhai, M.; Totolo, O.; Modisi, M.P.; Finkelman, R.B.; Kelesitse, S.M.; Menyatso, M. Heavy metal distribution in soils near Palapye, Botswana: An evaluation of the environmental impact of coal mining and combustion on soils in a semi-arid region. *Environ. Geoch. Health* **2009**, *31*, 759–770. [CrossRef]
72. Agrawal, P.; Mittal, A.; Prakash, R.; Kumar, M.; Singh, T.B.; Tripathi, S.K. Assessment of contamination of soil due to heavy metals around coal fired thermal power plants at Singrauli region of India. *Bull. Environ. Contam. Toxicol.* **2010**, *85*, 2019–2223. [CrossRef]
73. Raja, R.; Nayak, A.K.; Shukla, A.K.; Rao, K.S.; Gautam, P.; Lal, B.; Tripathi, R.; Shahid, M.; Panda, B.B.; Kumar, A.; et al. Impairment of soil health due to fly ash-fugitive dust deposition from coal-fired thermal power plants. *Environ. Monit. Assess.* **2015**, *187*, 679. [CrossRef]
74. Howladar, M.F.; Ahmed, T.; Deb, P.K.; Shine, F.M.M.; Rahman, M.A. Analysing the top soil chemistry for environments around the Barapukuria thermal power plant, Bangladesh. *Int. J. Sci. Eng. Res.* **2016**, *7*, 146–150.
75. Linnik, W.G.; Minkina, T.M.; Bauer, T.V.; Saveliev, A.A.; Mandzhieva, S.S. Geochemical assessment and spatial analysis of heavy metals pollution around coal-fired power station. *Environ. Geochem. Health* **2019**, *42*, 4087–4100. [CrossRef] [PubMed]

76. Lu, X.; Liu, W.; Zhao, C.; Chen, C. Environmental assessment of heavy metal and natural radioactivity in soil around a coal-fired power plant in China. *J. Radioanal. Nucl. Chem.* **2013**, *295*, 1845–1854. [CrossRef]
77. Hajduk, E.; Kaniuczak, J.; Właśniewski, S. The Content of Heavy Metals in Arable Soils from the Vicinity of the Stalowa Wola Power Plant. *Soil Sci. Annu.* **2012**, *63*, 22–26. [CrossRef]
78. Adeyi, A.A.; Torto, N. Profiling heavy metal distribution and contamination in soil of old power generation station in Lagos, Nigeria. *Am. J. Sci. Technol.* **2014**, *1*, 1–10.
79. Pastrana-Corral, M.A.; Wakida, F.T.; Temores-Peña, J.; Rodriguez-Mendivil, D.D.; García-Flores, E.; Piñon-Colin, T.D.J.; Quiñonez-Plaza, A. Heavy metal pollution in the soil surrounding a thermal power plant in Playas de Rosarito, Mexico. *Environ. Earth Sci.* **2017**, *76*, 583. [CrossRef]
80. Parzentny, H.R. Differences between the content of selected ecotoxic elements in feed coal, combustion residues, soils and common beech *(Fagus sylvatica* L.) in the surrounded of the power plant in Poland. *Int. Multidiscip. Sci. GeoConference SGEM.* **2019**, *19*, 271–293.
81. Duffus, J.H. "Heavy metals"—A meaningless term? (IUPAC Technical Report). *Pure Appl. Chem.* **2002**, *74*, 793–807. [CrossRef]
82. Dai, S.; Ren, D.; Chou, C.-L.; Finkelman, R.B.; Seredin, V.V.; Zhou, Y. Geochemistryof trace elements in Chinese coals: A review of abundances, genetic types, impactson human health, and industrial utilization. *Int. J. Coal Geol.* **2012**, *94*, 3–21. [CrossRef]
83. Ptak, B.; Różkowska, A. *Geochemical Atlas of Coal Deposits Upper Silesian Coal Basin*; Publishing of Polish Geological Institute: Warsaw, Poland, 1995; p. 53.
84. Parzentny, H.R.; Róg, L. Evaluation the value of some petrographic, physico-chemical and geochemical indicatores of quality of coal in paralic series of the Upper Silesian Coal Basin and attempt to find a correlotion between thrm. *Gospod. Miner. Resour. Manag.* **2017**, *33*, 51–76. (In Polish)
85. Parzentny, H.R.; Róg, L. Modes of occurrence of ecotoxic elements in coal from the Upper Silesian Coal Basin, Poland. *Arabian J. Geosci.* **2018**, *11*, 790. [CrossRef]
86. Parzentny, H.R.; Róg, L. Dependences between certain petrographic, geochemical and technological indicators of coal quality in the Limnic Series of the Upper Silesian Coal Basin (USCB), Poland. *Arch. Min. Sci.* **2020**, *65*, 665–684.
87. Masovian Voivodeship. Available online: https://pl.wikipedia.org/wiki/Wojew%C3%B3-dztwo_mazowieckie (accessed on 23 September 2020).
88. Upper Silesian Conurbation. In Wikipedia, the Free Encyclopedia. Available online: https://pl.wikipedia.org/wiki/Konurbacja_górnośląska (accessed on 23 September 2020).
89. Opole Voivodeship. Available online: https://pl.wikipedia.org/wiki/Wojew%C3%B3dztwo_opolskie (accessed on 23 September 2020).
90. The Main Wind Directions in Poland. Available online: https://www.google.com/search?source=-univ&tbm=isch&q=kierunki+wiatru+w+polsce&sa=X&ved=2ahUKEwjU9OTUqonsAhVwxIsKHbKhDHAQjJkEegQICRAB&biw=1280&bih=891 (accessed on 23 September 2020).
91. World Reference Base for soil resources. *World Soil Resour. Rep.* **2015**, *106*, 1–193.
92. Soil Survey Staff. *Keys to Soil Taxonomy*, 12th ed.; USDA Natural Resources Conservation Service: Washington, DC, USA, 2014; p. 633.
93. ISO 7404-3. *Methods for the Petrographic Analysis of Bituminous Coal and Anthracite—Part. 3: Method of Determining Maceral Group Composition*; International Organization for Standardization: Geneva, Switzerland, 2009; p. 7.
94. ISO 7404-5. *Methods for the Petrographic Analysis of Bituminous Coal and Anthracite—Part. 5: Method of Determining Microscopically the Reflectance of Vitrinite*; International Organization for Standardization: Geneva, Switzerland, 2009; p. 14.
95. Taylor, J.C. Computer programs for standardless quantitative analysis of minerals using the full powder diffraction profile. *Powder Diffr.* **1991**, *6*, 2–9. [CrossRef]
96. Rietveld, H.M. A profile refinement method for nuclear and magnetic structures. *J. Appl. Crystallogr.* **1969**, *2*, 65–71. [CrossRef]
97. Ruan, C.-D.; Ward, C.R. Quantitative X-ray powder diffraction analysis of clay minerals in Australian coals using Rietveld methods. *Appl. Clay Sci.* **2002**, *21*, 227–240. [CrossRef]
98. Mahieux, P.Y.; Aubert, J.E.; Cyr, M.; Coutand, C.; Husson, B. Quantitative mineralogical composition of complex mineral wastes—Contribution of the Rietveld method. *Waste Manag.* **2010**, *30*, 378–388. [CrossRef]
99. Guo, Z.X.; Geng, H.; Zhang, J.H.; Zhou, H.; Peng, Y.; Zhai, S.Y.; Li, J.L.; Chen, Y.S. Ecological and health risks of trace heavy metals in atmospheric $PM_{2.5}$ collected in Wuxiang Town, Shanxi Province. *Huan Jing Ke Xue* **2018**, *39*, 1004–1013. (In Chinese) [CrossRef]
100. Silva, L.F.O.; Oliveira, M.L.S.; da Boit, K.M.; Finkelman, R.B. Characterization of Santa Catarina (Brazil) coal with respect to human health and environmental concerns. *Environ. Geochem Health* **2009**, *31*, 475–485. [CrossRef]
101. Bureau Veritas Mineral Laboratories Schedule of Services Bro. Vancouver, Canada. 2020. Available online: http://acmelab.com (accessed on 23 September 2020).
102. The Regulation of the Minister of the Environment of 15 July 2011 on the criteria for the classification of extractive waste for inert waste. In *Polish Journal of Laws 2011 Item 1048*; The Regulation of the Minister of the Environment: Warsaw, Poland, 2011.
103. Directive 2006/21/EC of the European Parliament and of the Council of 15 March 2006 on the Management of Waste from Extractive Industries and Amanding Directive 2004/35/EC. Available online: http://www.legislation.gov.uk/eudr/2006/21/introduction (accessed on 23 September 2020).

104. The Regulation of the Minister of the Environment of 1 September 2016 on the assessment of the pollution of the earth's surface. In *Polish Journal of Laws 2016 Item 1395*; The Regulation of the Minister of the Environment: Warsaw, Poland, 2016.
105. Economic Commission for Europe; Committee on Sustainable Energy. *International Classification of in-Seam Coals*; United Nations Report Energy/1998/19; UN; UN: New York, NY, USA; Geneva, Switzerland, 1998.
106. Ratajczak, T.; Gaweł, A.; Górniak, K.; Muszyński, M.; Szydłak, T.; Wyszomirski, P. Characteristics of fly ash from combustion of some hard and brown coals. *Spec. Pap. Mineral. Soc. Pol.* **1999**, *15*, 1–34. (In Polish)
107. Wierońska, F.; Makowska, D.; Strugała, A.; Bytnar, K. Analysis of the content of nickel, chromium, lead and zinc in solid products of coal combustion (CCPs) coming from Polish power plants. *IOP Publ. IOP Conf. Ser. Earth Environ. Sci.* **2019**, *214*, 012029. [CrossRef]
108. Llorens, J.F.; Fernandez, J.L.; Querol, X. The fate of trace elements in a large coal-fired power plant. *Environ. Geol.* **2000**, *40*, 409–416. [CrossRef]
109. Karayiğit, A.I.; Yigitler, Ő.; İşerli, S.; Querol, X.; Mastalerz, M.; Oskay, G.; Hower, J.C. Mineralogy and Geochemistry of Feed Coals and Combustion Residues from Tunçbilek and Seyitömer Coal-Fired Power Plants in Western Turkey. *Coal Combust. Gasif. Prod.* **2019**, *11*, 18–31.
110. Wei, Q.; Song, W. Mineralogical and chemical characteristics of coal ashes from two high-sulfur coal-fired power plants in Wuhai, Inner Mongolia, China. *Minerals* **2020**, *10*, 323. [CrossRef]
111. Lin, W.; Wu, K.; Lao, Z.; Hu, W.; Lin, B.; Li, Y.; Fan, H.; Hu, J. Assessment of trace metal contamination and ecological risk in the forest ecosystem of dexing mining area in northeast Jianxi Province, China. *Ecotoxicol. Environ. Saf.* **2019**, *167*, 76–82. [CrossRef] [PubMed]
112. Mandal, A.; Sengupta, D. An assessment of soil contamination due to heavy metals around a coal-fired thermal power plant in India. *Environ. Geol.* **2006**, *51*, 409–420. [CrossRef]
113. Parzentny, H. Differences in content and bonding pattern of certain elements in coal of the Upper Silesian Caol Basin throughout a single seam pfofile). *PrzeglądGórniczy* **1989**, *45*, 17–21. (In Polish)
114. Parzentny, H. Lead distribution in coal and coaly shales in the Upper Silesian Coal Basin. *Geol. Quat.* **1994**, *38*, 43–58.
115. Parzentny, H.R. Spatial macroscale variability of the role of mineral matter in concentrating some trace elements in bituminous coal in a coal basin—a case study from the Upper Silesian Coal Basin in Poland. *Minerals* **2020**, *10*, 422. [CrossRef]
116. Hill, P.A. Vertical distribution of elements in Deposit No. 1, Hat Creek, British Columbia: A preliminary study. *Int. J. Coal Geol.* **1990**, *15*, 77–111. [CrossRef]
117. Mohanty, M.K.; Honaker, R.Q.; Mondal, K.; Paul, B.C.; Ho, K. Trace element reductions in fine coal using advanced physical cleaning. *Coal Prep.* **1998**, *19*, 195–211. [CrossRef]
118. Makowska, D.; Strugała, A.; Wierońska, F.; Włodek, A. Investigations of the effectiveness of lead disposal from hard coal trough the cleaning process. *E2S Web Conf.* **2016**, *10*, 00117. [CrossRef]
119. Chen, J.; Chen, P.; Yao, D.; Huang, W.; Tang, S.; Wang, W.; Liu, W.; Hu, Y.; Zhang, B.; Sha, J. Abundance, distribution, and modes of occurrence of uranium in Chinese Coals. *Minerals* **2017**, *7*, 239. [CrossRef]
120. Duan, P.; Wang, W.; Sang, S.; Tang, Y.; Ma, M.; Zhang, W.; Liang, B. Geochemistry of toxic elements and their removal via the preparation of high-uranium coal in Southwestern China. *Minerals* **2018**, *8*, 83. [CrossRef]
121. Liu, C.; Zhou, C.; Zhang, N.; Pan, J.; Cao, S.; Tang, M.; Ji, W.; Hu, T. Modes of occurrence and partitioning behavior of trace elements during coal preparation - A case study in Guizhou Province, China. *Fuel* **2019**, *243*, 79–87. [CrossRef]
122. Parzentny, H.R.; Lewińska-Preis, L. The role of sulphide and carbonate minerals in the concentration of chalcophile elements in the bituminous coal seams of a paralic series (Upper Carboniferous) in the Upper Silesian Coal Basin (USCB), Poland. *Chem. Erde Geochem.* **2006**, *66*, 227–247. [CrossRef]
123. Hower, J.C.; Campbell, J.L.; Teesdale, W.J.; Nejedly, Z.; Robertson, J.D. Scanning proton microprobe analysis of mercury and other trace elements in Fe-sulfides from a Kentucky coal. *Int. J. Coal Geol.* **2008**, *75*, 88–92. [CrossRef]
124. Diehl, S.F.; Goldhaber, M.B.; Koenig, A.E.; Lowers, H.A.; Ruppert, L.F. Distribution of arsenic, selenium, and other trace elements in high pyrite Appalachian coals: Evidence for multiple episodes of pyrite formation. *Int. J. Coal Geol.* **2012**, *94*, 238–249. [CrossRef]
125. Bai, X.; Wang, Y.; Li, W. Mineralogy, distribution, occurrence and removability of trace elements during the coal preparation of No. 6 coal from Heidaigou mine. *Int. J. Coal Sci. Technol.* **2014**, *1*, 402–420. [CrossRef]
126. Kokowska-Pawłowska, M. Petrographic and mineral variability of the rocks accompanying selected coal seams of the Poruba beds and their influenceof the trace elements content. *Gospod. Surowcami Miner. Miner. Resour. Manag.* **2015**, *31*, 73–92.
127. Bielowicz, B.; Misiak, J. The forms of occurrence and geochemistry of sulfides in hard coal deposits of the Libiąż Beds in the Upper Silesian Coal Basin, Southern Poland. *Geol. Geophys. Environ.* **2017**, *43*, 109–125. [CrossRef]
128. Kolker, A.; Finkelman, R.B. Potentially hazardous elements in coal: Modes of occurrence and summary of concentration data for coal components. *Int. J. Coal Prep. Util.* **1998**, *19*, 133–157. [CrossRef]
129. Kolker, A. Minor element distribution in iron disulfides in coal: A geochemical review. *Int. J. Coal Geol.* **2012**, *94*, 32–43. [CrossRef]
130. Jiang, Y.; Qian, H.; Zhou, G. Mineralogy and geochemistry of different morphological pyrite in Late Permian coals, South Chin. *Arab. J. Geosci.* **2016**, *9*, 590. [CrossRef]
131. Deditius, A.P.; Utsunomiya, S.; Reich, M.; Kesler, S.E.; Ewing, R.C.; Hough, R.; Walshe, J. Trace metal nanoparticles in pyrite. *Ore Geol. Rev.* **2011**, *42*, 32–46. [CrossRef]

132. Adamczyk, Z.; Nowińska, K. Chemical composition of pyrite in the feed mixture into zinc and lead pirometallurgical process. In *Support Systems in Production Engineering Geochemistry and Environmental Geology of Industrial Areas*; Pozzi, M., Ed.; "Panova" Publishing House: Gliwice, Poland, 2016; Volume 5, pp. 38–46. (In Polish)
133. Reich, M.; Deditius, A.; Chryssoulius, S.; Li, J.-W.; Ma, C.-Q.; Parada, M.A.; Barra, F.; Mittemayr, F. Pyrite as a record of hydrothermal fluid evolution in a porphyry copper system: A SIMS/EMPA trace element study. *Geoch. Cosmoch. Acta* **2013**, *104*, 42–62. [CrossRef]
134. Serranti, S.; Ferrini, V.; Masi, U.; Cabri, L.J. Trace-element distribution in cassiterite and sulfides from Rubané and massive ores of the Corvo deposit, Portugal. *Can. Mineral.* **2002**, *40*, 815–835. [CrossRef]
135. Dare, S.A.S.; Barnes, S.; Beaudoin, G.; Méric, J.; Boutroy, E.; Potvin-Doucet, C. Trace elements in magnetite as petrogenetic indicators. *Miner. Depos.* **2014**, *49*, 785–796. [CrossRef]
136. Wang, Y.; Zhu, W.; Zhong, H.; Bai, Z.; Yao, J.; Xu, C. Using trace elements of magnetite to constrain the origin of the Pingchuan hydrothermal low-Ti magnetite deposit in the Panxi area, SW China. *Acta Geochim.* **2019**, *38*, 376–390. [CrossRef]
137. Vassilev, S.V.; Eskenazy, G.M.; Vassileva, C.G. Behaviour of elements and minerals during preparation and combustion of the Pernik coal, Bulgaria. *Fuel Proc. Technol.* **2001**, *72*, 103–129. [CrossRef]
138. Wang, J.; Yang, Z.; Quin, S.; Panchal, B.; Sun, Y.; Niu, H. Distribution characteristics and migration patterns of hazardous trace elements in coal combustion products of power plants. *Fuel* **2019**, *258*, 116062. [CrossRef]
139. Parzentny, H.R.; Róg, L. Distribution of heavy metals in fly ash originating from burning coal of Upper Silesian Coal Basin. *Przegląd Górniczy* **2001**, *57*, 52–60. (In Polish)
140. Misz, M.A. Comparasion of chars in slag and fly ash as formed in pf boilers from Będzin Power Station (Poland). *Fuel* **2002**, *81*, 1351–1358. [CrossRef]
141. Sokol, E.V.; Kalugin, V.M.; Nigmatulina, E.N.; Volkova, N.I.; Frenkel, A.E.; Maksimova, N.V. Ferrospheres from fly ashes of Chelyabinsk coals: Chemical composition, morphology and formation conditions. *Fuel* **2002**, *81*, 867–876. [CrossRef]
142. Wilczyńska-Michalik, W.; Moryl, R.; Sobczyk, J.; Michalik, M. Composition of coal combustion by-products: The importance of combustion technology. *FuelProc. Tech.* **2014**, *124*, 35–43. [CrossRef]
143. Valentim, B.; Shreya, N.; Paul, B.; Gomes, C.S.; Sant'Ovaia, H.; Guedes, A.; Ribeiro, J.; Flores, D.; Pinho, S.; Suárez-Ruiz, I.; et al. Characteristics of ferrospheres in fly ashes derived from Bokaro and Jharia (Jharkand, India) coals. *Int. J. Coal Geol.* **2016**, *153*, 52–74. [CrossRef]
144. Hower, J.C.; Cantando, E.; Eble, C.F.; Copley, G.C. Characterization of stoker ash from the combustion of high-lanthanide coal at a Kentucky bourbon distillery. *Int. J. Coal Geol.* **2019**, *213*, 103260. [CrossRef]
145. Hower, J.C.; Qian, D.; Briot, N.J.; Santillan-Jimenez, E.; Hood, M.M.; Taggart, R.K.; Hsu-Kim, H. Nano-scale rare earth distribution in fly ash derived from the combustion of the fire clay coal, kentucky. *Minerals* **2019**, *9*, 206. [CrossRef]
146. Maity, R.; Venkateshwarlu, M.; Mondal, S.; Kapawar, M.R.; Gain, D.; Paul, P. Magnetic and microscopic characterization of anthropogenically produced magnetic particles: A proxy for environmental pollution. *Int. J. Environ. Sci. Technol.* **2020**, *114*. [CrossRef]
147. Xu, M.; Yan, R.; Zheng, C.; Oiao, Y.; Han, J.; Sheng, C. Status of trace element emission in a coal combustion process: A review. *Fuel Proc. Techn.* **2003**, *85*, 215–237. [CrossRef]
148. The Engineering ToolBox. Melting and Boiling Temperatures—Evaporation and Melting Heats of Common Materials. Available online: https://www.engineeringtoolbox.com/melting-boiling-temperatures-d_392.html (accessed on 23 September 2020).
149. Bartoňová, L.; Raclavská, H.; Čech, B.; Kucbel, M. Behavior of Pb during coal combustion: An overview. *Sustainability* **2019**, *11*, 6061. [CrossRef]
150. Chen, G.; Sun, Y.; Wang, Q.; Yan, B.; Cheng, Z.; Ma, W. Partitioning of trace elements in coal combustion products: A comparative study of different applications in China. *Fuel* **2019**, *240*, 31–39. [CrossRef]
151. Cui, W.; Meng, Q.; Feng, Q.; Zhou, L.; Cui, Y.; Li, W. Occurrence and release of cadmium, chromium, and lead from stone coal combustion. *Int. J. Coal Sci Technol.* **2019**, *6*, 586–594. [CrossRef]
152. Vassileva, C.G.; Vassilev, S.V. Behaviour of inorganic matter during heting of Bulgarian coals. 2. Subbiltuminous and bituminous coals. *Fuel Proc. Technol.* **2006**, *87*, 1095–1116. [CrossRef]
153. Magiera, T.; Parzentny, H.R.; Róg, L.; Chybiorz, R.; Wawer, M. Spatial variation of soil magnetic susceptibility in relation to different emission sources in southern Poland. *Geoderma* **2015**, *255–256*, 94–103. [CrossRef]
154. Magiera, T.; Mendakiewicz, M.; Szuszkiewicz, M.; Jabłońska, M.; Chróst, L. Technogenic magnetic particles in soils as evidence of historical mining and smelting activity: A case of the Brynica River Valley, Poland. *Sci. Total Environ.* **2016**, *566–567*, 536–551. [CrossRef]
155. Strzyszcz, Z.; Magiera, T. Heavy metal contamination and magnetic susceptibility in soils of southern Poland. *Phys. Chem. Earth* **1998**, *23*, 1127–1131. [CrossRef]
156. Jordanova, N.; Jordanova, D.; Tsacheva, T. Application of magnetometry for delineation of anthropogenic pollution in areas covered by various soil types. *Geoderma* **2008**, *144*, 557–571. [CrossRef]
157. Minkina, T.; Konstatinova, E.Y.; Bauer, T.V.; Mandzhieva, S.S.; Sushkova, S.N.; Chapligin, V.A.; Burachevskaya, M.V.; Nazarenko, O.; Kizilkaya, R.; Gülser, C.; et al. Environmental and human health risk assessment of potentially toxic elements in soils around the largest coal-fired power station in Southern Russia. Environ. *Geoch. Health.* **2020**. [CrossRef]

158. Kapper, K.L.; Bautista, F.; Goguitchaishvili, A.; Bógalo, M.F.; Cejudo-Ruíz, R.; Cervantes, S.M. The use and misuse of magnetic methods to monitor environmental pollution in urban areas. *Boletín Soc. Geológica Mex.* **2020**, *72*, 1–44. [CrossRef]
159. Yean, S.; Cong, L.; Yavuz, C.T.; Mayo, J.T.; Yu, W.W.; Kan, A.T.; Colvin, V.L.; Tomson, M.B. Effect of magnetite particle size on adsorption and desorption of arsenite and arsenate. *J. Mater. Res.* **2005**, *20*, 3255–3264. [CrossRef]
160. Usman, M.; Byrne, M.; Chaundhary, A.; Orsetti, S.; Hanna, K.; Ruby, C.; Kappler, A.; Haderalein, S.B. Magnetite and green rust: Synthesis, properties, and environmental applications of mixed-valent iron minerals. *Chem. Rev.* **2018**, *118*, 3251–3304. [CrossRef] [PubMed]
161. Ajmal, Z.; Usman, M.; Anastopoulos, I.; Qadeer, A.; Zhu, R.; Wakeel, A.; Dong, R. Use of nano-/micro-magnetite for abatement of cadmium and lead contamination. *J. Environ. Manag.* **2020**, *264*, 110477. [CrossRef] [PubMed]
162. Kukier, U.; Ishak, C.F.; Sumner, M.E.; Miller, W.P. Composition and element solubility of magnetic and non-magnetic fly ash fractions. *Environ. Pollut.* **2003**, *123*, 255–266. [CrossRef]
163. Seferenioğlu, M.; Paul, M.; Sandström, Å.; Köker, A.; Toprak, S.; Paul, J. Acid leaching of coal and coal-ashes. *Fuel* **2003**, *82*, 1721–1734. [CrossRef]
164. Brownfield, M.E.; Cathcart, J.D.; Aolter, R.H.; Brownfield, I.K.; Rice, C.A.; O'Connor, J.T.; Zielinski, J.R.A.; Bullock, J.H.; Hower, J.C.; Meeker, G.P. *Characterization and Modes of Occurrence of Elements in Feed Coal and Coal Combustion Products from a Power Plant. Utilizing Low-Sulfur Coal from the Powder River Basin, Wyoming*; Scientific Investigations Report 2004-5271; U.S. Geological Survey: Reston, VA, USA, 2005; p. 36. Available online: http://pubs.usgs.gov/sir/2004/5271/ (accessed on 23 September 2019).
165. Vassilev, S.V.; Baxter, D.; Andersen, L.K.; Vassileva, C.G. An overview of the chemical composition of biomass. *Fuel* **2010**, *89*, 913–933. [CrossRef]
166. Niemiec, M.; Chowaniak, M.; Paluch, Ł. Accumulation of chromium, aluminum, barium and arsenic in selected elements of a forest ecosystem in the Przedbabiogórskie Mountain Range in the Western Carpathians. *J. Elem.* **2017**, *22*, 1107–1116.
167. Parzentny, H.; Róg, L. Importance of geological conditions for industry development on area between Bytom and Katowice. *PrzeglądGórniczy* **1999**, *56*, 26–34. (In Polish)
168. Pająk, M.; Jasik, M. The level of Zn, Cd and Pb accumulation in top layer of forest soil in the neighbourhood of metallurgic complex "MiasteczkoSląskie". Scientific Journals of the University of Zielona Góra No. 137. *Environ. Eng.* **2010**, *17*, 112–122. (In Polish)
169. Adamczyk, Z.; Nowińska, K. Environmental mobility of trace elements present in dusts emitted from Zn–Pb metallurgical processes. *Environ. Earth. Sci.* **2016**, *75*, 956. [CrossRef]
170. Walthert, L.; Pannatier, E.G.; Meier, E.S. Shortage of nutrients and excess of toxic elements in soils limit the distribution of soil-sensitive tree species in temperate forests. *Forest Ecol. Manag.* **2013**, *297*, 94–107. [CrossRef]
171. Brunner, I.; Luster, J.; Günthardt-Goerg, M.S.; Frey, B. Heavy metal accumulation and phytostabilisation potential of tree fine roots in a contaminated soil. *Environ. Pollut.* **2008**, *152*, 559–568. [CrossRef] [PubMed]
172. Akburak, S. Variations of element concentrations in roots of different tree species. *Cerne* **2020**, *26*, 118–129. [CrossRef]
173. Kidd, P.; Barceló, J.; Bernal, M.P.; Navari-Izzo, F.; Poschenrieder, C.; Shilev, S.; Clemente, R.; Monterroso, C. Trace element behaviour at the root–soil interface: Implications in phytoremediation. *Environ. Exp. Bot.* **2009**, *67*, 243–259. [CrossRef]
174. Antoniadis, V.; Levizou, E.; Shaheen, S.M.; Ok, Y.S.; Sebastian, A.; Baum, C.; Prasad, M.N.V.; Wenzel, W.W.; Rinklebe, J. Trace elements in the soil-plant interface: Phytoavailability, translocation, and phytoremediation—A review. *Earth Sci. Rev.* **2017**, *171*, 621–645. [CrossRef]